Martinec, Z., Hagedoorn, J. (2014): The rotational feedback on linear-momentum balance in glacial isostatic adjustment.- *Geophysical Journal International*, *199*, 3, p. 1823-1846

DOI: http://doi.org/10.1093/gji/ggu369

Geophysical Journal International

Geophys. J. Int. (2014) **199,** 1823–1846 doi: 10.1093/gji/ggu369
GJI Gravity, geodesy and tides

The rotational feedback on linear-momentum balance in glacial isostatic adjustment

Zdeněk Martinec[1,2] and Jan Hagedoorn[3,4]

[1] *Dublin Institute for Advanced Studies, 5 Merrion Square, Dublin 2, Ireland. E-mail: zdenek@cp.dias.ie*
[2] *Department of Geophysics, Faculty of Mathematics and Physics, Charles University, V Holešovičkách 2,* 180 00 *Prague 8, Czech Republic*
[3] *Department for Geodesy and Geoinformation Sciences, Technical University of Berlin, Straße des 17. Juni* 135, *D-*10623 *Berlin, Germany*
[4] *Department of Geodesy and Remote Sensing, German Research Centre for Geosciences, D-*14473, *Potsdam, Germany*

Accepted 2014 September 17. Received 2014 September 17; in original form 2014 May 12

SUMMARY

The influence of changes in surface ice-mass redistribution and associated viscoelastic response of the Earth, known as glacial isostatic adjustment (GIA), on the Earth's rotational dynamics has long been known. Equally important is the effect of the changes in the rotational dynamics on the viscoelastic deformation of the Earth. This signal, known as the rotational feedback, or more precisely, the rotational feedback on the sea level equation, has been mathematically described by the sea level equation extended for the term that is proportional to perturbation in the centrifugal potential and the second-degree tidal Love number.

The perturbation in the centrifugal force due to changes in the Earth's rotational dynamics enters not only into the sea level equation, but also into the conservation law of linear momentum such that the internal viscoelastic force, the perturbation in the gravitational force and the perturbation in the centrifugal force are in balance. Adding the centrifugal-force perturbation to the linear-momentum balance creates an additional rotational feedback on the viscoelastic deformations of the Earth. We term this feedback mechanism, which is studied in this paper, as the rotational feedback on the linear-momentum balance.

We extend both the time-domain method for modelling the GIA response of laterally heterogeneous earth models developed by Martinec and the traditional Laplace-domain method for modelling the GIA-induced rotational response to surface loading by considering the rotational feedback on linear-momentum balance. The correctness of the mathematical extensions of the methods is validated numerically by comparing the polar-motion response to the GIA process and the rotationally induced degree 2 and order 1 spherical harmonic component of the surface vertical displacement and gravity field. We present the difference between the case where the rotational feedback on linear-momentum balance is considered against that where it is not. Numerical simulations show that the resulting difference in radial displacement and sea level change between these situations since the Last Glacial Maximum reaches values of ± 25 and ± 1.8 m, respectively. Furthermore, the surface deformation pattern is modified by up to 10 per cent in areas of former or ongoing glaciation, but by up to 50 per cent at the bottom of the southern Indian ocean. This also results in the movement of coastlines during the last deglaciation to differ between the two cases due to the difference in the ocean loading, which is seen for instance in the area around Hudson Bay, Canada and along the Chinese, Australian or Argentinian coastlines.

Key words: Sea level change; Geopotential theory; Earth rotation variations.

1 INTRODUCTION

The redistribution of ice and water over the Earth's surface during glaciation and deglaciation cycles due to changes in climate induces 3-D crustal motion, gravity-field variations and changes in sea level, which is known collectively as glacial isostatic adjustment (GIA). The surface-mass redistribution and associated mass redistribution in the Earth's interior are capable of perturbing the rotation of the Earth, both in direction and magnitude of the rotation vector. A wander of the rotation axis induces a perturbation in the centrifugal force, which acts, in turn, as an additional load. This loading is manifested in all GIA-related observables, that is crustal motions, sea level variations and the

perturbations in the gravity potential (e.g. Milne & Mitrovica 1996; Mitrovica *et al.* 2001), and is known as the rotational feedback (Peltier 1998).

The secular changes of the Earth's rotation axis during ice ages over timescales of 1 Myr has been intensively investigated over the past two and a half decades. Han & Wahr (1989) were the first to consider the effect of GIA-induced change in the rotation vector on sea level, while Milne & Mitrovica (1996) first derived a complete, gravitationally self-consistent extension of the sea level equation to include the rotational-feedback mechanism, see also Milne & Mitrovica (1998), Peltier (1999) and Mitrovica *et al.* (2001). The spatial and temporal pattern of GIA-related observables due to the feedback mechanism was successively refined by, for example, Peltier (1999), Mitrovica *et al.* (2001, 2005), Peltier & Luthcke (2009), Peltier & Drummond (2010), Mitrovica & Wahr (2011) and Roy & Peltier (2011). While this shows that a deep insight into the physics of the induced wander of the rotation axis for a deforming and rotating Earth has been attempted, despite the significant scientific effort, the mutual coupling between the Earth's deformation caused by ice-mass loading and the induced wander of rotation axis is still under scientific debate (e.g. Chambers *et al.* 2010, 2012; Métivier *et al.* 2012; Peltier *et al.* 2012).

The rotational feedback on sea level is mathematically described by adding an extra term into the sea level equation that is proportional to the GIA-induced perturbations in the centrifugal potential and the second-degree tidal Love number (Milne & Mitrovica 1996, 1998; Peltier 1998, 1999; Mitrovica *et al.* 2001). Since the sea level equation describes the spatial and temporal distribution of the ocean-water load, the additional term modifies the loading and subsequently induces additional crustal deformation and gravity-field perturbations. Due to the reason that follows, we refine the notion introduced by Peltier (1998) and will refer to this effect as the rotational feedback on the sea level equation. As this feedback mechanism has been intensively studied in the literature, we will not deal with it in this paper.

The perturbation in the centrifugal force enters not only into the sea level equation, but also into the conservation law of linear momentum such that the internal contact (or surface) viscoelastic force, the perturbation in the gravitational force and the perturbation in the centrifugal force are in balance. Since the perturbation in the centrifugal force results from the rotational response of a deforming Earth to surface loading, this additional contribution to a solution of the linear-momentum balance can also be viewed as a rotational feedback. To distinguish it from the rotational feedback in the sea level equation, we will refer to this as the rotational feedback on the linear-momentum balance.

To extend the existing theories for modelling the GIA signal by rotational feedback on the linear-momentum balance, we will proceed in two steps. First, the time-domain (TD) method for modelling the GIA response of laterally heterogeneous earth models developed by Martinec (2000) will be extended by adding the perturbation in the centrifugal force into the linear-momentum equation. Simultaneously, Poisson's equation for the perturbation in the gravitational potential will be extended by adding the perturbation in centrifugal potential. These two partial differential equations will be coupled with the linearized Liouville equation for the GIA-induced rotational response of the Earth. A non-trivial part in this step is the derivation of the boundary condition for the perturbation in gravity potential at the Earth's surface and on the core–mantle boundary. The extended TD method will be checked against the traditional Laplace-domain (LD) method for computing the polar-motion response $m(t)$ to the GIA process (e.g. Wu & Peltier 1984). The numerical agreement between the extended TD method and the LD method for the time evolution of $m(t)$ will numerically validate the correctness of the mathematical formulation of the TD method extended for the rotational feedback in linear-momentum balance.

In the second step, we generalize the traditional LD method (Wu & Peltier 1984) for an additional term in the gravitational-potential boundary condition which arises due to the rotational feedback on the linear-momentum balance. The generalization concerns the time evolution of the rotationally induced degree 2 and order 1 spherical harmonic component of displacement and gravity potential. The numerical agreement with the extended TD method will validate the mathematical correctness of the extended LD method. At this stage, the TD and LD methods will be considered to be fully mathematically consistent. Finally, we show the difference between the case where the rotational feedback on linear-momentum balance is included against the case without this feedback mechanism.

The main objective of the paper is to present the theoretical extension of the TD and LD methods for the rotational feedback on the linear-momentum balance in a transparent way. That is why we will not consider the rotational feedback on the sea level equation, but our surface load model will be defined by a simple spherical cap used by Spada *et al.* (2011) for a benchmark study of the numerical performance of GIA computational codes. This provides the rotational amplitudes and the rotational relaxation times of the M3L70V01 model (Spada *et al.* 2011) for the case where the rotational-feedback mechanism is included, which may then serve as a benchmark for other GIA computational codes. A full exploitation of the rotational-feedback effect on the complete suite of GIA-related observables, including the rotational feedback on the sea level equation, is the next step for future study.

2 THE INITIAL HYDROSTATIC EQUILIBRIUM

We treat the Earth as a self-gravitating deformable body, which is composed of a fluid core and a laterally heterogeneous viscoelastic solid mantle, separated from each other by the core–mantle boundary. Let the Earth be in mechanical equilibrium at time $t = 0$ and rotate about its centre of mass O with the uniform angular velocity $\vec{\Omega}_0$. We will use this initial equilibrium configuration κ_0 as the reference configuration for the description of both the wander of the rotational axis and the motion inside the deformed Earth induced by time-varying external surface-mass loading. We choose a Cartesian coordinate system $O(x_1, x_2, x_3)$ corotating with the Earth, such that the coordinate axes x_1, x_2, x_3 coincide with the principal axes of inertia of the configuration κ_0. Let A, B and C ($A = B < C$) be the corresponding principal moments of inertia. We suppose that the axis of uniform rotation of the equilibrium configuration κ_0 coincides with the axis of the largest principal moment of inertia, so that $\vec{\Omega}_0 = \Omega_0 \vec{e}_3$, where $\vec{e}_3$ is the Cartesian unit base vector in the x_3 direction. A material particle in κ_0 is assigned

by its position vector $\vec{x}$, measured in the uniformly rotating reference frame $O(x_1, x_2, x_3)$. Let V be the volume of the Earth in the initial configuration κ_0 and $\varrho_0(\vec{x})$ be the volume-mass density in V. The inertia tensor of the configuration κ_0, as viewed in the corotating frame $O(x_1, x_2, x_3)$, may be written as the volume integral (e.g. Moritz & Mueller 1987)

$$\boldsymbol{C}_0 = \int_V \varrho_0(\vec{x})\,[(\vec{x}\cdot\vec{x})\boldsymbol{I} - \vec{x}\otimes\vec{x}]\,\mathrm{d}V(\vec{x}), \tag{1}$$

where the dot and cross denote the scalar and dyadic product of vectors, respectively, and $\boldsymbol{I}$ is the second-order identity tensor.

In the gravitating and rotating Earth, there are two volume forces acting on a material particle. The attractive gravitational force per unit mass, $-\mathrm{grad}\,\phi_0$, generated by the volume-mass density $\varrho_0(\vec{x})$ and represented by the gravitational potential $\phi_0(\vec{x})$ and the repulsive centrifugal force per unit mass, $-\mathrm{grad}\,\psi_0$, represented by the centrifugal potential $\psi_0(\vec{x})$ and appearing since a rotating frame is used as the reference for the description of the deformation of the Earth and the motion of its rotation axis.

The gravitational potential $\phi_0(\vec{x})$ in the initial equilibrium satisfies Poisson's equation,

$$\nabla^2\phi_0 = 4\pi G\varrho_0 \quad \text{in } V, \tag{2}$$

together with the continuity conditions

$$[\phi_0]^+_- = 0, \qquad [\vec{n}\cdot\mathrm{grad}\,\phi_0]^+_- = 0 \quad \text{on } \partial V \cup \Sigma, \tag{3}$$

where G is Newton's gravitational constant, ∂V and Σ are the Earth's surface and an internal discontinuity across which the unperturbed density $\varrho_0(\vec{x})$ exhibits a finite jump (including the core–mantle boundary ∂C), respectively. A unit normal to either ∂V or Σ is denoted by $\vec{n}$. The symbol $[f]^+_-$ denotes the jump of quantity f on ∂V or Σ and a superscript $+$ $(-)$ denotes the evaluation of f on the external (internal) side of ∂V or Σ.

The centrifugal potential $\psi_0(\vec{x})$ in the initial equilibrium

$$\psi_0(\vec{x}) = -\frac{1}{2}\left[\Omega_0^2(\vec{x}\cdot\vec{x}) - (\vec{\Omega}_0\cdot\vec{x})^2\right] \tag{4}$$

is continuous at the internal discontinuity Σ,

$$[\psi_0]^+_- = 0 \quad \text{on } \Sigma, \tag{5}$$

but vanishes outside the Earth,

$$\psi_0^+ = 0 \quad \text{on } \partial V, \tag{6}$$

where ψ_0^+ denotes the centrifugal potential on the external side of ∂V.

The sum of the two forces, the so-called the gravity force per unit mass, can be represented as the negative gradient of the gravity potential $\Phi_0 = \phi_0 + \psi_0$. The gravity potential $\Phi_0(\vec{x})$ satisfies Poisson's equation

$$\nabla^2\Phi_0 = 4\pi G\varrho_0 - 2\Omega_0^2 \quad \text{in } V, \tag{7}$$

together with the continuity conditions

$$[\Phi_0]^+_- = 0, \qquad [\vec{n}\cdot\mathrm{grad}\,\Phi_0]^+_- = 0 \quad \text{on } \Sigma, \tag{8}$$

and the inhomogeneous boundary conditions

$$\left.\begin{aligned} \Phi_0^- &= \phi_0^+ + \psi_0^-, \\ \vec{n}\cdot\mathrm{grad}\,\Phi_0^- &= \vec{n}\cdot\mathrm{grad}\,\phi_0^+ + \vec{n}\cdot\mathrm{grad}\,\psi_0^- \end{aligned}\right\} \quad \text{on } \partial V. \tag{9}$$

The initial static stress $\boldsymbol{t}_0(\vec{x})$ is assumed to be hydrostatic, $\boldsymbol{t}_0 = -p_0(\vec{x})\boldsymbol{I}$ everywhere in V, where $p_0(\vec{x})$ is the initial hydrostatic pressure. The mechanical equilibrium of the uniformly rotating Earth is then reduced to the hydrostatic equilibrium where the compression due to gravity is balanced by a pressure gradient. The balance of these two forces is guaranteed by the equation of hydrostatic equilibrium

$$\mathrm{grad}\,p_0 + \varrho_0\,\mathrm{grad}\,\Phi_0 = \vec{0} \quad \text{in } V. \tag{10}$$

The boundary condition associated with eq. (10) is $[p_0]^+_- = 0$ on Σ. In particular, $p_0^- = 0$ on ∂V, where p_0^- denotes the initial pressure on the internal side of ∂V.

3 APPLICATION OF A SURFACE-MASS LOAD

3.1 Inertia-tensor increments

We assume that a time- and space-varying surface-mass load is applied to the Earth's surface ∂V at $t = 0+$ and deforms the initial hydrostatic configuration κ_0 into the time-dependent instantaneous configuration $\kappa(t)$. Let $O(t)$ be the centre of mass of the configuration $\kappa(t)$. We will

require that the position of $O(t)$ with respect to the rotating frame $O(x_1, x_2, x_3)$ does not change in time and coincides with the centre of mass O of the configuration κ_0, that is $O(t) \equiv O$ at any time $t > 0$. By $\vec{r}(\vec{x}, t)$, we denote the instantaneous position of a particle in the configuration $\kappa(t)$ initially located at the position $\vec{x}$ in the configuration κ_0. The position $\vec{r}(\vec{x}, t)$ can be represented by the displacement $\vec{u}(\vec{x}, t)$ of the particle $\vec{x}$ from its equilibrium position

$$\vec{r}(\vec{x}, t) = \vec{x} + \vec{u}(\vec{x}, t). \tag{11}$$

As introduced, we assume that the deformation of the Earth is induced by the redistribution of surface masses. Correct to first order in $\|\vec{u}\|$, the instantaneous inertia tensor $\boldsymbol{c}^{\mathrm{L}}(t)$ associated with a time-varying surface-mass load, as viewed in the rotating frame $O(x_1, x_2, x_3)$, can be linearized as (Martinec & Hagedoorn 2005, eq. 16)

$$\boldsymbol{c}^{\mathrm{L}}(t) = \int_{\partial V} \sigma^{\mathrm{L}}(\vec{x}, t)\,[(\vec{x}\cdot\vec{x})\boldsymbol{I} - \vec{x}\otimes\vec{x}\,]\,\mathrm{d}S(\vec{x}), \tag{12}$$

where $\sigma^{\mathrm{L}}(\vec{x}, t)$, $\vec{x} \in \partial V$, is the surface-mass density of the load measured with respect to undeformed unit area $\mathrm{d}S(\vec{x})$ and the label L stands for 'Load'. The rotational response of the Earth to the surface load is described by the instantaneous inertia tensor $\boldsymbol{C}^{\mathrm{R}}(t)$ of the configuration $\kappa(t)$. Correct to first order in $\|\vec{u}\|$, the tensor $\boldsymbol{C}^{\mathrm{R}}(t)$, as viewed in the rotating frame $O(x_1, x_2, x_3)$, can be linearized as (Martinec & Hagedoorn 2005, eqs 13 and 14)

$$\boldsymbol{C}^{\mathrm{R}}(t) = \boldsymbol{C}_0 + \boldsymbol{c}^{\mathrm{R}}(t), \tag{13}$$

where the label R stands for 'Response' and the inertia-tensor increment $\boldsymbol{c}^{\mathrm{R}}(t)$ has the form

$$\boldsymbol{c}^{\mathrm{R}}(t) \int_V \varrho_0(\vec{x})\,[2\,(\vec{x}\cdot\vec{u}(\vec{x}, t))\,\boldsymbol{I} - \vec{x}\otimes\vec{u}(\vec{x}, t) - \vec{u}(\vec{x}, t)\otimes\vec{x}\ ]\,\mathrm{d}V(\vec{x}). \tag{14}$$

The total increment $\boldsymbol{c}(t)$ of the initial inertial tensor $\boldsymbol{C}_0$ is then expressed as the sum of two constituents,

$$\boldsymbol{c}(t) = \boldsymbol{c}^{\mathrm{L}}(t) + \boldsymbol{c}^{\mathrm{R}}(t). \tag{15}$$

3.2 Motion of rotation axis

The instantaneous angular velocity $\vec{\omega}(t)$ of the configuration $\kappa(t)$, as viewed in the rotating frame $O(x_1, x_2, x_3)$, can be decomposed into the uniform angular velocity $\vec{\Omega}_0$ and a small perturbation $\Omega_0\vec{m}(t)$:

$$\vec{\omega}(t) = \vec{\Omega}_0 + \Omega_0\vec{m}(t). \tag{16}$$

The dimensionless quantities $m_1(t)$ and $m_2(t)$ express the deviations of the instantaneous rotation axis from its equilibrium position and the quantity $m_3(t)$ characterizes variations in the rotational speed.

The motion of the rotation axis of the current configuration $\kappa(t)$ is governed by the principle of angular-momentum conservation which results in the Liouville equation for parameters $\vec{m}(t)$ (Munk & MacDonald 1960; Moritz & Mueller 1987). Assuming that the inertia-tensor increment $\boldsymbol{c}(t)$, the relative angular-momentum vector $\vec{h}(t)$ and the rotation parameters $\vec{m}(t)$ of the configuration $\kappa(t)$ are small quantities whose product may be neglected, the Liouville equation can be linearized, and subsequently solved by direct time integration. For the quantity $m_3(t)$, the integration gives

$$m_3(t) = -\frac{1}{C\Omega_0}\,[\Omega_0 c_{33}(t) + h_3(t)]\,, \tag{17}$$

where $c_{33}(t)$ and $h_3(t)$ are the Cartesian components of the inertia-tensor increment $\boldsymbol{c}(t)$ and the relative angular-momentum vector $\vec{h}(t)$, respectively.

The wander of the rotation vector induced by a non-oscillatory long-term redistribution of the surface-mass load consists of periodic oscillations with the Chandler-wobble frequency superimposed on long-term variations. The Chandler wobbling of the rotation vector can be removed by moving-average filtering of $m(t)$ over the Chandler-wobble period [as conventional, we will use a complex notation and define $m(t) = m_1(t) + \mathrm{i}\,m_2(t)$]. As a result, long-term motion of the rotation vector is expressed as (Wu & Peltier 1984; Vermeersen & Sabadini 1996; Mitrovica & Milne 1998; Martinec & Hagedoorn 2005)

$$m(t) = \chi(t), \tag{18}$$

where the complex polar-motion excitation function is defined by

$$\chi(t) = \frac{1}{(C-A)\Omega_0}\,[\Omega_0 c(t) + h(t)]\,, \tag{19}$$

and $c(t) = c_{13}(t) + \mathrm{i}\,c_{23}(t)$ and $h(t) = h_1(t) + \mathrm{i}\,h_2(t)$.

4 EULERIAN POTENTIAL INCREMENTS

4.1 The Eulerian density increment

Time changes in the volume-mass density in the instantaneous configuration $\kappa(t)$ can be described by the Eulerian increment ϱ^{E} of the unperturbed mass density (e.g. Wolf 1991; Dahlen & Tromp 1998):

$$\varrho^{\mathrm{E}} = \varrho(\vec{r}, t) - \varrho_0\,[\vec{x}(\vec{r}, t)]\,. \tag{20}$$

This increment can be expressed in terms of the displacement $\vec{u}(\vec{x}, t)$ by linearizing the mass-conservation law (Martinec & Hagedoorn 2005, eq. 47),

$$\varrho^{\mathrm{E}} = -\mathrm{div}\left[\varrho_0(\vec{x})\vec{u}(\vec{x}, t)\right], \tag{21}$$

which is correct to a first order in $\|\vec{u}\|$. Since it is irrelevant in linearized theory whether the increment ϱ^{E} is regarded as a function of $\vec{r}$ or $\vec{x}$, we consider ϱ^{E} to depend on the position vector $\vec{x}$, that is $\varrho^{\mathrm{E}}(\vec{x}, t)$.

As traditional in GIA modelling, the effect of a fluid core on the Earth's viscoelastic response to long-term glacial loading is modelled by a static-deformation approximation (Dahlen 1974; Crossley & Gubbins 1975). In view of this concept, the Eulerian density increment in the fluid core is

$$\varrho^{\mathrm{E}} = \frac{\vec{n}\cdot\mathrm{grad}\,\varrho_0}{\vec{n}\cdot\mathrm{grad}\,\Phi_0}\,\Phi^{\mathrm{E}}, \tag{22}$$

where $\vec{n}$ is the unit normal to a level surface Σ of density ϱ_0 and gravity potential Φ_0 in the initial configuration κ_0 and Φ^{E} is the Eulerian gravity-potential increment (see Section 4.4). Moreover, in GIA modelling, it is justifiable to approximate the unperturbed density of the fluid core by an average value of the PREM density stratification of the core (Dziewonski & Anderson 1981). Klemann (personal communication, 2007) tested the validity of this assumption against the case where the Earth is modelled by a full viscoelastic sphere with the PREM core stratification of the unperturbed density and with a low viscosity of 5×10^{19} Pa s. The comparison of the viscoelastic responses of the full-sphere model against the spherical-shell model where the effect of the core is approximated by static deformation with a constant unperturbed density shows that the relative difference is of the order of 5×10^{-3} for spherical harmonic degree $j = 2$ of the Eulerian gravity-potential increment, with the error decreasing with increasing spherical harmonic degree. This relative error is acceptable since it is of the same order as the error associated with the spherical approximation applied in GIA modelling (Martinec & Hagedoorn 2005, section 4.2). Hence, adopting the static-deformation approximation of a fluid core and assuming a constant unperturbed density of the core implies that the Eulerian density increment vanishes in the core, $\varrho^{\mathrm{E}} = 0$.

4.2 The Eulerian gravitational-potential increment

As a response to the time changes in the volume-mass density distribution, the gravitational potential $\phi(\vec{r}, t)$ of the configuration $\kappa(t)$ changes over time, which may be described by the Eulerian increment ϕ^{E} of the initial gravitational potential, that is by the quantity

$$\phi^{\mathrm{E}} = \phi(\vec{r}, t) - \phi_0[\vec{x}(\vec{r}, t)]. \tag{23}$$

The increment ϕ^{E} satisfies the following boundary-value problem (e.g. Dahlen & Tromp 1998):

$$\nabla^2\phi^{\mathrm{E}} = 4\pi G\,\varrho^{\mathrm{E}} \quad \text{in } V - \Sigma \tag{24}$$

subject to the interface conditions on an internal discontinuity Σ:

$$\left.\begin{aligned}\left[\phi^{\mathrm{E}}\right]^{+}_{-} &= 0\\ \left[\vec{n}\cdot\mathrm{grad}\,\phi^{\mathrm{E}}\right]^{+}_{-} &= -4\pi G\sigma^{\Sigma}\end{aligned}\right\} \quad \text{on } \Sigma, \tag{25}$$

and the boundary conditions on the external boundary ∂V:

$$\left.\begin{aligned}\left[\phi^{\mathrm{E}}\right]^{+}_{-} &= 0\\ \left[\vec{n}\cdot\mathrm{grad}\,\phi^{\mathrm{E}}\right]^{+}_{-} &= 4\pi G\sigma^{\partial V} + 4\pi G\sigma^{\mathrm{L}}\end{aligned}\right\} \quad \text{on } \partial V. \tag{26}$$

Outside the volume V, the Eulerian density increment ϱ^{E} vanishes and the incremental gravitational potential is harmonic, $\nabla^2\phi^{\mathrm{E}} = 0$. The surface-mass densities $\sigma^{\Sigma}(\vec{x}, t)$ and $\sigma^{\partial V}(\vec{x}, t)$ are defined by

$$\begin{aligned}\sigma^{\Sigma}(\vec{x}, t) &= [\varrho_0(\vec{x})\,(\vec{n}(\vec{x})\cdot\vec{u}(\vec{x}, t))]^{+}_{-} \quad \text{for } \vec{x}\ \in \Sigma,\\ \sigma^{\partial V}(\vec{x}, t) &= \varrho_0(\vec{x}^{-})\left(\vec{n}(\vec{x})\cdot\vec{u}(\vec{x}^{-}, t)\right) \quad \text{for } \vec{x}\ \in \partial V\end{aligned} \tag{27}$$

and $\varrho_0(\vec{x}^{-})$ and $\vec{u}(\vec{x}^{-}, t)$ denote the volume-mass density and the displacement, respectively, on the interior side of ∂V.

4.3 The Eulerian centrifugal-potential increment

Time changes in the size and orientation of the instantaneous angular velocity $\vec{\omega}(t)$ induce perturbations in the centrifugal potential. These may be described by the Eulerian increment ψ^{E} of the initial centrifugal potential:

$$\psi^{\mathrm{E}} = \psi(\vec{r}, t) - \psi_0[\vec{x}(\vec{r}, t)]. \tag{28}$$

Substituting the centrifugal potentials of the initial equilibrium configuration κ_0 and the instantaneous configuration $\kappa(t)$, respectively, the increment ψ^{E} can be expressed as a function of the rotational parameters m_i. In terms of the zeroth- and second-degree spherical harmonics, this expression, correct to a first order in m_i, is (e.g. Martinec & Hagedoorn 2005, eqs 94 and 95)

$$\psi^{\mathrm{E}}(\vec{x}, t) = r^2 \psi^{\mathrm{E}}_{00}(t) Y_{00}(\Omega) + r^2 \sum_{m=-1}^{1} \psi^{\mathrm{E}}_{2m}(t) Y_{2m}(\Omega), \tag{29}$$

where

$$\begin{aligned} \psi^{\mathrm{E}}_{00}(t) &= -\frac{4}{3}\sqrt{\pi}\,\Omega_0^2 m_3(t), \qquad \psi^{\mathrm{E}}_{20}(t) = -\frac{1}{\sqrt{5}}\psi^{\mathrm{E}}_{00}(t), \\ \psi^{\mathrm{E}}_{21}(t) &= -\sqrt{\frac{2\pi}{15}}\,\Omega_0^2 m^*(t), \qquad \psi^{\mathrm{E}}_{2,-1}(t) = -\left[\psi^{\mathrm{E}}_{21}(t)\right]^*. \end{aligned} \tag{30}$$

Differentiating ψ^{E} with respect to r yields

$$\vec{e}_{\mathrm{r}} \cdot \mathrm{grad}\, \psi^{\mathrm{E}} = \frac{2}{r}\psi^{\mathrm{E}}, \tag{31}$$

where $\vec{e}_{\mathrm{r}}$ is the unit vector in the radial direction. Moreover, the application of the Laplace operator to eq. (29) results in

$$\nabla^2 \psi^{\mathrm{E}} = -4\Omega_0^2 m_3 \quad \text{in } V. \tag{32}$$

As introduced earlier, the earth model consists of a fluid core and a solid viscoelastic mantle separated from each other by the core–mantle boundary. For GIA modelling, we will assume that there is no differential rotation between the fluid core and the mantle and that the core corotates with the mantle. This means that the centrifugal potential ψ passes continuously through the core–mantle boundary. We also assume that ψ is continuous at a mantle discontinuity Σ. To express this condition mathematically, let the internal discontinuity Σ in the initial configuration κ_0 be moved to the discontinuity $\sigma(t)$ in the current configuration $\kappa(t)$ by internal deformations. The continuity of the centrifugal potential ψ at the displaced point $\vec{r}$ on the deformed discontinuity $\sigma(t)$ is expressed as

$$\left[\psi\right]^+_- = 0 \quad \text{on } \sigma(t). \tag{33}$$

Taking into account the decomposition (28) and the fact that the initial equilibrium centrifugal potential ψ_0 is continuous on the deformed discontinuity $\sigma(t)$, we find that the Eulerian centrifugal-potential increment ψ^{E} passes continuously through discontinuity $\sigma(t)$. In addition, correct to a first order in $\|\mathrm{grad}\, \vec{u}\|$, the continuity of ψ^{E} on $\sigma(t)$ can be viewed as the continuity of ψ^{E} on the undeformed discontinuity Σ, that is

$$\left[\psi^{\mathrm{E}}\right]^+_- = 0 \quad \text{on } \Sigma. \tag{34}$$

However, the continuity of the centrifugal potential is not valid at the Earth surface since the centrifugal force vanishes outside the Earth, causing the continuity condition (34) to reduce to

$$\psi^{\mathrm{E}+} = 0 \quad \text{on } \partial V, \tag{35}$$

where $\psi^{\mathrm{E}+}$ denotes the centrifugal-potential increment on the external side of ∂V.

4.4 The Eulerian gravity-potential increment

Time variations of both the gravitational and centrifugal potentials due to the mass redistribution on the Earth's surface and inside the Earth, and associated changes in the Earth's rotation dynamics mean that the gravity potential $\Phi(\vec{r}, t) = \phi(\vec{r}, t) + \psi(\vec{r}, t)$ of the configuration $\kappa(t)$ also varies in time. This can be described by the Eulerian increment Φ^{E} of the initial gravity potential:

$$\Phi^{\mathrm{E}} = \Phi(\vec{r}, t) - \Phi_0[\vec{x}(\vec{r}, t)]. \tag{36}$$

In view of eqs (23) and (28), the Eulerian gravity-potential increment Φ^{E} is equal to the sum of the Eulerian gravitational-potential increment ϕ^{E} and the Eulerian centrifugal-potential increment ψ^{E}, that is

$$\Phi^{\mathrm{E}} = \phi^{\mathrm{E}} + \psi^{\mathrm{E}}. \tag{37}$$

By considering eqs (24) and (32), Φ^{E} satisfies Poisson's equation of the form

$$\nabla^2 \Phi^{\mathrm{E}} = 4\pi G \varrho^{\mathrm{E}} - 4\Omega_0^2 m_3 \quad \text{in } V - \Sigma. \tag{38}$$

The interface conditions (25) and (34) combine to give

$$\left.\begin{aligned} \left[\Phi^{\mathrm{E}}\right]^{+}_{-} &= 0 \\ \left[\vec{n}\cdot\operatorname{grad}\Phi^{\mathrm{E}}\right]^{+}_{-} &= -4\pi G\sigma^{\Sigma} \end{aligned}\right\} \quad \text{on } \Sigma, \tag{39}$$

where the surface-mass density σ^{Σ} is given by eq. $(27)_1$. Likewise, the boundary conditions (26) and (35) yield

$$\left.\begin{aligned} \Phi^{\mathrm{E}-} &= \phi^{\mathrm{E}+} + \psi^{\mathrm{E}-} \\ \vec{n}\cdot\operatorname{grad}\Phi^{\mathrm{E}-} &= \vec{n}\cdot\operatorname{grad}\phi^{\mathrm{E}+} + \vec{n}\cdot\operatorname{grad}\psi^{\mathrm{E}-} - 4\pi G\sigma^{\partial V} - 4\pi G\sigma^{\mathrm{L}} \end{aligned}\right\} \quad \text{on } \partial V, \tag{40}$$

where the surface-mass density $\sigma^{\partial V}$ is given by eq. $(27)_2$.

5 GLACIAL ISOSTASY ON A ROTATING EARTH

5.1 Extended differential-equation formulation

We are dealing with the viscoelastic response of a self-gravitating, deformable earth model to a surface-mass load, and intend to extend the traditional theory of viscoelastic relaxation (e.g. Farrell 1972; Wu & Peltier 1982) to the case where the Earth is rotating and its rotational dynamics is changing as a response to a change in surface loading. As introduced, we assume that the Earth rotates with a constant angular velocity $\vec{\Omega}_0$ prior applying the surface-mass load and with a time-varying angular velocity $\vec{\omega}(t)$ as the surface-mass load changes.

After applying a time-varying mass load with surface density σ^{L} to the external surface ∂V, the response of a viscoelastic earth model B is governed by the conservation of linear momentum (inertial forces are neglected) and by Poisson's equation for small perturbations of a hydrostatically pre-stressed and self-gravitating continuum in a rotating reference frame $O(x_1, x_2, x_3)$,

$$\left.\begin{aligned} \operatorname{div}\boldsymbol{\tau} - \varrho_0\operatorname{grad}\Phi^{\mathrm{E}} + \operatorname{grad}(\varrho_0\vec{u}\cdot\vec{g}_0) + \varrho^{\mathrm{E}}\vec{g}_0 &= 0 \\ \nabla^2\Phi^{\mathrm{E}} - 4\pi G\varrho^{\mathrm{E}} &= -4\Omega_0^2 m_3 \end{aligned}\right\} \quad \text{in } B, \tag{41}$$

where $\boldsymbol{\tau}$ is the Lagrangian increment of the Cauchy stress tensor and $\vec{g}_0$ is the initial gravity, $\vec{g}_0 = -\operatorname{grad}\Phi_0$. Eqs (41) are derived by applying the incremental field theory (e.g. Wu & Peltier 1982; Wolf 1991), which allows us to adopt the assumption of a spherical approximation (Martinec & Hagedoorn 2005, section 4.2). This means that (i) the Earth is represented by a sphere B with the unit normal to the external surface ∂V and an internal discontinuity Σ coinciding with the unit radial vector $\vec{e}_{\mathrm{r}}$, $\vec{n} = \vec{e}_{\mathrm{r}}$, and (ii) the unperturbed mass density ϱ_0 is radially dependent only, that is $\varrho_0 = \varrho_0(r)$.

We should emphasize that the centrifugal-force increment $\operatorname{grad}\psi^{\mathrm{E}}$ is included in the linear-momentum balance via the gravity-force increment $\operatorname{grad}\Phi^{\mathrm{E}}$ and the centrifugal-potential increment ψ^{E} in Poisson's equation via the gravity-potential increment Φ^{E}. These two additional terms extend the traditional differential-equation formulation of GIA (e.g. Farrell 1972; Wu & Peltier 1982) where only the gravitational-force increment $\operatorname{grad}\phi^{\mathrm{E}}$ and the gravitational-potential increment ϕ^{E} are considered.

As discussed in Section 4.1, the effect of a fluid core on the Earth's viscoelastic response to long-term glacial loading is viewed in terms of a static deformation. This concept allows us to consider the solution domain B as a solid viscoelastic spherical shell, representing the Earth's mantle, bounded by a fluid–solid boundary ∂C, representing the core–mantle boundary, and by the surface ∂V, representing the Earth's surface. Thus, the surface ∂B bounding the solution domain B consists of two parts, $\partial B = \partial C \cup \partial V$.

The boundary conditions on the external surface ∂V vary over time and are functions of the time evolution of the surface-mass load changes. They are therefore of the form

$$\left.\begin{aligned} \vec{e}_{\mathrm{r}}\cdot\boldsymbol{\tau}^{-}\cdot\vec{e}_{\mathrm{r}} &= -g_0(a)\sigma^{\mathrm{L}} \\ \boldsymbol{\tau}^{-}\cdot\vec{e}_{\mathrm{r}} - \left(\vec{e}_{\mathrm{r}}\cdot\boldsymbol{\tau}^{-}\cdot\vec{e}_{\mathrm{r}}\right)\vec{e}_{\mathrm{r}} &= \vec{0} \\ \Phi^{\mathrm{E}-} &= \phi^{\mathrm{E}+} + \psi^{\mathrm{E}-} \\ \frac{1}{4\pi G}\operatorname{grad}\Phi^{\mathrm{E}-}\cdot\vec{e}_{\mathrm{r}} + \varrho_0^{-}(\vec{u}^{-}\cdot\vec{e}_{\mathrm{r}}) &= \frac{1}{4\pi G}\left(\operatorname{grad}\phi^{\mathrm{E}+}\cdot\vec{e}_{\mathrm{r}} + \frac{2}{a}\psi^{\mathrm{E}-}\right) - \sigma^{\mathrm{L}} \end{aligned}\right\} \quad \text{on } \partial V, \tag{42}$$

where a is the radius of ∂V and $g_0(a)$ is the magnitude of $\vec{g}_0$ on ∂V. The symbols $\boldsymbol{\tau}^{-}$, ϱ_0^{-} and $\vec{u}^{-}$ denote the stress tensor increment, the unperturbed mass density and the displacement on the interior side of ∂V, respectively. The first pair of boundary conditions on the traction increment can be found in Longman (1963) or Farrell (1972), whereas the second pair of boundary conditions on the Eulerian gravity-potential increment and the Eulerian gravity-force increment follow from eq. (40) by the substitution from eqs $(27)_2$ and (31).

To complete the formulation, the boundary conditions for the displacement, the traction increment, the gravity potential and the gravity intensity increments are prescribed at an internal discontinuity Σ (e.g. Dahlen 1974), and eq. (39):

$$\left.\begin{aligned} [\vec{u}]^+_- &= 0 \\ [\boldsymbol{\tau}\cdot\vec{e}_{\rm r}]^+_- &= 0 \\ \left[\Phi^{\rm E}\right]^+_- &= 0 \\ \left[\frac{1}{4\pi G}\,\mathrm{grad}\,\Phi^{\rm E}\cdot\vec{e}_{\rm r}+\varrho_0(\vec{u}\cdot\vec{e}_{\rm r})\right]^+_- &= 0 \end{aligned}\right\} \quad \text{on } \Sigma. \tag{43}$$

Since an inviscid fluid core is included, the continuity of the normal component of the displacement, that is, $\vec{e}_{\rm r}\cdot\vec{u}$, the continuity of the normal component of the stress vector, that is, $\vec{e}_{\rm r}\cdot\boldsymbol{\tau}\cdot\vec{e}_{\rm r}$ and the free-slip behaviour, that is, $\boldsymbol{\tau}\cdot\vec{e}_{\rm r}-(\vec{e}_{\rm r}\cdot\boldsymbol{\tau}\cdot\vec{e}_{\rm r})\vec{e}_{\rm r}=\vec{0}$, are appropriate, instead of eq. (43). These conditions can be expressed in the form (e.g. Chinnery 1975; Tromp & Mitrovica 1999), and eq. (39):

$$\left.\begin{aligned} \left[\vec{u}\cdot\vec{e}_{\rm r}\right]^+_- &= 0 \\ \vec{e}_{\rm r}\cdot\boldsymbol{\tau}^+-\varrho_0^-\left[g_0(b)(\vec{u}\cdot\vec{e}_{\rm r})+\Phi^{\rm E}\right]\vec{e}_{\rm r} &= \vec{0} \\ \left[\Phi^{\rm E}\right]^+_- &= 0 \\ \frac{1}{4\pi G}\left[\mathrm{grad}\,\Phi^{\rm E}\cdot\vec{e}_{\rm r}\right]^+_- + [\varrho_0]^+_-(\vec{u}\cdot\vec{e}_{\rm r}) &= 0 \end{aligned}\right\} \quad \text{on } \partial C, \tag{44}$$

where b is the radius of ∂C and $g_0(b)$ is the magnitude of $\vec{g}_0$ on ∂C. The symbols $\boldsymbol{\tau}^+$ and ϱ_0^- denote the stress tensor increment and the unperturbed mass density on ∂C from the mantle and core side, respectively.

Provided that the spatial-time variations of the surface-mass load $\sigma^{\rm L}$ and temporal variations of the polar motion (m_1, m_2) and rotation speed m_3 are specified, the above initial, boundary-value problem describes the spatiotemporal behaviour of the displacement field $\vec{u}$ and the Eulerian gravity-potential increment $\Phi^{\rm E}(=\phi^{\rm E}+\psi^{\rm E})$ as independent field variables. In what follows, our strategy of solving this problem will make use of existing numerical methods applied to solve the associated problem for a non-rotating Earth. In this particular case, the Eulerian centrifugal-potential increment $\psi^{\rm E}$ is identically equal to zero and the Eulerian gravity-potential increment $\Phi^{\rm E}$ is reduced to the Eulerian gravitational-potential increment $\phi^{\rm E}$. Moreover, the rotation parameters m_i, $i=1,2,3$, are also identically equal to zero, the non-homogeneous Poisson's equation $(41)_2$ is reduced to a homogeneous one, and the non-homogeneous boundary conditions $(42)_{3,4}$ are reduced by terms proportional to $\psi^{\rm E}$. Finally, the unperturbed gravity potential Φ_0 is reduced to the unperturbed gravitational potential ϕ_0.

5.2 Weak formulation

The initial, boundary-value problem (41)–(44) for a non-rotating Earth has been formulated in a weak sense by Martinec (2000). We will now modify this formulation for a rotating Earth by adding the perturbation in the centrifugal potential into eqs (41)–(44).

As introduced, the Eulerian gravitational-potential increment $\phi^{\rm E}$ considered by Martinec (2000) as an independent field variable for a non-rotating Earth is now replaced by the Eulerian gravity-potential increment $\Phi^{\rm E}$ for a rotating Earth. Under such a replacement, the forms of the differential equations and the boundary conditions expressed in terms of $\phi^{\rm E}$ (and $\vec{u}$) for a non-rotating Earth are the same as those expressed in terms of $\Phi^{\rm E}$ (and $\vec{u}$) for a rotating Earth. The only difference is that the right-hand side of Poisson's equation $(41)_2$ vanishes for a non-rotating Earth and the boundary condition $(42)_{3,4}$ do not contain the two terms depending on $\psi^{\rm E}$. Hence, the modification of the weak formulation concerns how to extend the original weak formulation such that these additional terms are accounted for.

Following the considerations by Martinec (2000), for functions $(\vec{u},\,\Phi^{\rm E},\,\Pi)$ from an appropriate functional space $V_{\rm sol}$, whose detailed specification is given by Martinec (2000, eq. 27), let us define the energy functional $\mathcal{E}$ by the sum of the term $\mathcal{E}_{\rm press}$ associated with the pressure, elastic shear energy $\mathcal{E}_{\rm shear}$, gravity energy $\mathcal{E}_{\rm gravity}$ and the term $\mathcal{E}_{\rm uniq}$ associated with the uniqueness of a solution:

$$\mathcal{E}(\vec{u},\,\Phi^{\rm E},\,\Pi)=\mathcal{E}_{\rm press}(\vec{u},\,\Pi)+\mathcal{E}_{\rm shear}(\vec{u})+\mathcal{E}_{\rm gravity}(\vec{u},\,\Phi^{\rm E})+\mathcal{E}_{\rm uniq}(\vec{u}), \tag{45}$$

where the energy constituents are, except $\mathcal{E}_{\rm gravity}$ and $\mathcal{E}_{\rm uniq}$, defined by Martinec (2000, eqs 30–32). For a rotating Earth, the original gravitational energy $\mathcal{E}_{\rm grav}$ of the form

$$\mathcal{E}_{\rm grav}(\vec{u},\,\phi^{\rm E})=\mathcal{E}^{\rm (I)}_{\rm grav}(\vec{u})+\frac{1}{8\pi G}\int_B\left(\mathrm{grad}\,\phi^{\rm E}\cdot\mathrm{grad}\,\phi^{\rm E}\right)\mathrm{d}V+\int_B\varrho_0(\vec{u}\cdot\mathrm{grad}\,\phi^{\rm E})\mathrm{d}V, \tag{46}$$

where $\mathcal{E}^{\rm (I)}_{\rm grav}(\vec{u})$ is given by Martinec (2000, eq. A1), is now replaced by the gravity energy $\mathcal{E}_{\rm gravity}$. This energy can be derived from the gravitational energy, provided that the Eulerian gravitational-potential increment $\phi^{\rm E}$ is replaced by the Eulerian gravity-potential increment $\Phi^{\rm E}$

$$\mathcal{E}_{\rm gravity}(\vec{u},\,\Phi^{\rm E})=\mathcal{E}^{\rm (I)}_{\rm grav}(\vec{u})+\frac{1}{8\pi G}\int_B\left(\mathrm{grad}\,\Phi^{\rm E}\cdot\mathrm{grad}\,\Phi^{\rm E}\right)\mathrm{d}V+\int_B\varrho_0(\vec{u}\cdot\mathrm{grad}\,\Phi^{\rm E})\mathrm{d}V. \tag{47}$$

The six conditions on vanishing a rigid-body translation and rotation are derived in (Martinec & Hagedoorn 2005, section 2.4). These conditions ensure that the position of the centre of mass is fixed during GIA process and the relative angular-momentum vector $\vec{h}(t)$ vanishes. They are used to define the term $\mathcal{E}_{\rm uniq}$ in a similar way as eq. (33) in Martinec (2000).

Moreover, we introduce the linear functional $\mathcal{F}^{i+1}$ taken at the current time t^{i+1} by the sum of the dissipative term taken at the previous time t^i, the term associated with the boundary conditions on traction increment, the term associated with the boundary condition on the Eulerian gravity increment and the term associated with the source term on the right-hand side of Poisson's equation $(41)_2$ (all three later terms are taken at the current time t^{i+1}):

$$\mathcal{F}^{i+1}(\vec{u},\,\Phi^{\rm E}) = \mathcal{F}^{i}_{\rm diss}(\vec{u}) + \mathcal{F}^{i+1}_{\rm surf}(\vec{u}) + \mathcal{F}^{i+1}_{\rm surf}(\Phi^{\rm E}) + \mathcal{F}^{i+1}_{\rm rot}(\Phi^{\rm E}), \tag{48}$$

where the first two terms on the right-hand side are given by Martinec (2000, eq. 35 and the first part of eq. 36), and the third term is chosen in the form

$$\mathcal{F}^{i+1}_{\rm surf}(\Phi^{\rm E}) = \int_{\partial B} b_1^{i+1}\,\Phi^{\rm E}{\rm d}S, \tag{49}$$

where an auxiliary variable b_1, taken at the current time t^{i+1}, is introduced to satisfy the boundary conditions $(42)_4$ and $(44)_4$ for the Eulerian gravity increment on ∂B, and the fourth term has the form

$$\mathcal{F}^{i+1}_{\rm rot}(\Phi^{\rm E}) = \int_{B} \varrho^{\rm CF}\Phi^{\rm E}{\rm d}V, \tag{50}$$

where $\varrho^{\rm CF} = \Omega_0^2 m_3/\pi G$.

The 'weak formulation' of the initial, boundary-value problem (41)–(44) consists of finding the fields $(\vec{u},\,\Phi^{\rm E},\,\Pi)$ from the functional space $V_{\rm sol}$ that fulfils a homogeneous initial condition and, at a fixed time, they satisfy the following variational equality:

$$\delta\mathcal{E}(\vec{u},\,\Phi^{\rm E},\,\Pi,\,\delta\vec{u},\,\delta\Phi^{\rm E},\,\delta\Pi) = \delta\mathcal{F}(\delta\vec{u},\,\delta\Phi^{\rm E}) \quad \forall(\delta\vec{u},\,\delta\Phi^{\rm E},\,\delta\Pi)\in V_{\rm sol}. \tag{51}$$

Note that we drop, in contrast to Martinec (2000), time labels i and $i+1$ since they are redundant in the following considerations. The variation of the energy constituents are, except for $\delta\mathcal{E}_{\rm gravity}$, given by Martinec (2000, eqs 40–43). The missing term reads as

$$\begin{aligned}\delta\mathcal{E}_{\rm gravity}(\vec{u},\,\Phi^{\rm E},\,\delta\vec{u},\,\delta\Phi^{\rm E}) = \delta\mathcal{E}^{\rm (I)}_{\rm grav}(\vec{u},\,\delta\vec{u}) + \frac{1}{4\pi G}\int_B \left(\operatorname{grad}\Phi^{\rm E}\cdot\operatorname{grad}\delta\Phi^{\rm E}\right){\rm d}V \\ + \int_B \varrho_0\left(\vec{u}\cdot\operatorname{grad}\delta\Phi^{\rm E}\right){\rm d}V + \int_B \varrho_0\left(\vec{\delta u}\cdot\operatorname{grad}\Phi^{\rm E}\right){\rm d}V.\end{aligned} \tag{52}$$

Likewise, the variation of the linear function $\mathcal{F}^{i+1}$ is

$$\delta\mathcal{F}^{i+1}(\delta\vec{u},\,\delta\Phi^{\rm E}) = \delta\mathcal{F}^{i}_{\rm diss}(\delta\vec{u}) + \delta\mathcal{F}^{i+1}_{\rm surf}(\delta\vec{u}) + \delta\mathcal{F}^{i+1}_{\rm surf}(\delta\Phi^{\rm E}) + \delta\mathcal{F}^{i+1}_{\rm rot}(\delta\Phi^{\rm E}), \tag{53}$$

where the first two terms on the right-hand side are given by Martinec (2000, eq. 45 and the first part of eq. 46), and the last two terms read as

$$\delta\mathcal{F}^{i+1}_{\rm surf}(\delta\Phi^{\rm E}) = \int_{\partial B} b_1^{i+1}\,\delta\Phi^{\rm E}{\rm d}S, \tag{54}$$

and

$$\delta\mathcal{F}^{i+1}_{\rm rot}(\delta\Phi^{\rm E}) = \int_{B} \varrho^{\rm CF}\delta\Phi^{\rm E}{\rm d}V. \tag{55}$$

To show that the weak formulation generalizes the differential-equation formulation of the problem (41)–(44), let us temporarily assume that the weak solution $(\vec{u},\,\Phi^{\rm E},\,\Pi)$ is sufficiently smooth such that the Green's theorems (Martinec 2000, eqs 50 and 51) can be applied to the second and the third integral on the right-hand side of eq. (52), respectively:

$$\begin{aligned}\delta\mathcal{E}_{\rm gravity}(\vec{u},\,\Phi^{\rm E},\,\delta\vec{u},\,\delta\Phi^{\rm E}) = \delta\mathcal{E}^{\rm (I)}_{\rm grav}(\vec{u},\,\delta\vec{u}) + \frac{1}{4\pi G}\Bigg[-\int_B \nabla^2\Phi^{\rm E}\delta\Phi^{\rm E}\,{\rm d}V + \int_{\partial B}\left(\vec{n}\cdot\operatorname{grad}\Phi^{\rm E}\right)\delta\Phi^{\rm E}\,{\rm d}S - \int_\Sigma\left[\vec{n}\cdot\operatorname{grad}\Phi^{\rm E}\right]^+_-\delta\Phi^{\rm E}\,{\rm d}S\Bigg] \\ - \int_B \operatorname{div}(\varrho_0\vec{u})\,\delta\Phi^{\rm E}\,{\rm d}V + \int_{\partial B}\varrho_0\,(\vec{n}\cdot\vec{u})\,\delta\Phi^{\rm E}\,{\rm d}S - \int_\Sigma\left[\varrho_0\,(\vec{n}\cdot\vec{u})\right]^+_-\delta\Phi^{\rm E}\,{\rm d}S + \int_B\varrho_0(\vec{\delta u}\cdot\operatorname{grad}\Phi^{\rm E}){\rm d}V.\end{aligned} \tag{56}$$

We modify the variational equality (Martinec 2000, eq. 52) by replacing $\delta\mathcal{E}_{\rm gravity}$ by $\delta\mathcal{E}_{\rm grav}$ and $\Phi^{\rm E}$ by $\phi^{\rm E}$, respectively. Then the implication of Martinec (2000, eq. 53) applied to the modified variational equality provides the Maxwell viscoelastic constitutive equation, the divergence-free constraint on displacement $\vec{u}$, the linear-momentum balance $(41)_1$, Poisson's equation $(41)_2$ and the interface conditions (43).

Moreover, the inspection of the modified variational equality shows that there are three surface integrals over the bounding surface ∂B that are proportional to the test function $\delta\Phi^{\rm E}$:

$$\frac{1}{4\pi G}\int_{\partial B}\left(\vec{n}\cdot\operatorname{grad}\Phi^{\rm E}\right)\delta\Phi^{\rm E}\,{\rm d}S + \int_{\partial B}\varrho_0\,(\vec{n}\cdot\vec{u})\,\delta\Phi^{\rm E}\,{\rm d}S = \int_{\partial B} b_1\,\delta\Phi^{\rm E}\,{\rm d}S, \tag{57}$$

where an auxiliary variable b_1 has been introduced to satisfy the boundary conditions $(42)_4$ and $(44)_4$ for the Eulerian gravity increment. In view of $\partial B = \partial C \cup \partial V$, we have

$$\frac{1}{4\pi G}\int_{\partial C}\left(\vec{n}\cdot\operatorname{grad}\Phi^{\mathrm{E}}\right)\delta\Phi^{\mathrm{E}}\,\mathrm{d}S+\int_{\partial C}\varrho_0\,(\vec{n}\cdot\vec{u})\,\delta\Phi^{\mathrm{E}}\,\mathrm{d}S+\frac{1}{4\pi G}\int_{\partial V}\left(\vec{n}\cdot\operatorname{grad}\Phi^{\mathrm{E}}\right)\delta\Phi^{\mathrm{E}}\,\mathrm{d}S+\int_{\partial V}\varrho_0\,(\vec{n}\cdot\vec{u})\,\delta\Phi^{\mathrm{E}}\,\mathrm{d}S$$
$$=\int_{\partial C}b_1\,\delta\Phi^{\mathrm{E}}\,\mathrm{d}S+\int_{\partial V}b_1\,\delta\Phi^{\mathrm{E}}\,\mathrm{d}S. \tag{58}$$

Since $\delta\Phi^{\mathrm{E}}$ is an arbitrary, infinitely differentiable function that does not vanish on ∂C nor on ∂V, then, according to the implication of Martinec (2000, eq. 54), the last integral equation can only be fulfilled if

$$\frac{1}{4\pi G}\vec{n}\cdot\operatorname{grad}\Phi^{\mathrm{E}}(b^+)+\varrho_0(b^+)\vec{n}\cdot\vec{u}(b^+)=b_1^{\partial C}, \tag{59}$$

$$\frac{1}{4\pi G}\vec{n}\cdot\operatorname{grad}\Phi^{\mathrm{E}}(a^-)+\varrho_0(a^-)\vec{n}\cdot\vec{u}(a^-)=b_1^{\partial V}, \tag{60}$$

where $b_1^{\partial C}$ and $b_1^{\partial V}$ denote the function b_1 on ∂C and ∂V, respectively. With the unit outward normal $\vec{n}$ to ∂V and ∂C equal to $\vec{e}_{\mathrm{r}}$ and $-\vec{e}_{\mathrm{r}}$, respectively, we then have

$$\frac{1}{4\pi G}\vec{e}_{\mathrm{r}}\cdot\operatorname{grad}\Phi^{\mathrm{E}}(b^+)+\varrho_0(b^+)\vec{e}_{\mathrm{r}}\cdot\vec{u}(b^+)=-b_1^{\partial C}, \tag{61}$$

$$\frac{1}{4\pi G}\vec{e}_{\mathrm{r}}\cdot\operatorname{grad}\Phi^{\mathrm{E}}(a^-)+\varrho_0(a^-)\vec{e}_{\mathrm{r}}\cdot\vec{u}(a^-)=b_1^{\partial V}. \tag{62}$$

However, the boundary-value functions $b_1^{\partial C}$ and $b_1^{\partial V}$ have not yet been specified. The requirement that the weak formulation for sufficiently smooth functions is equivalent to the differential-equation formulation now implies that $b_1^{\partial C}$ and $b_1^{\partial V}$ are chosen such that the boundary conditions $(44)_4$ and $(42)_4$ must be satisfied. The comparison of eqs $(44)_4$ and $(42)_4$ with eqs (61) and (62), respectively, implies that the functions $b_1^{\partial C}$ and $b_1^{\partial V}$ must be chosen in the form

$$b_1^{\partial C}=-\frac{1}{4\pi G}\left(\operatorname{grad}\Phi^{\mathrm{E}-}\cdot\vec{e}_{\mathrm{r}}\right)-\varrho_0^-(\vec{u}^+\cdot\vec{e}_{\mathrm{r}}), \tag{63}$$

where ϱ_0^- and $\Phi^{\mathrm{E}-}$ are the unperturbed density and the Eulerian gravity-potential increment on ∂C on the core side, respectively, and

$$b_1^{\partial V}=\frac{1}{4\pi G}\left(\operatorname{grad}\phi^{\mathrm{E}+}\cdot\vec{e}_{\mathrm{r}}+\frac{2}{a}\psi^{\mathrm{E}-}\right)-\sigma^{\mathrm{L}}, \tag{64}$$

where $\phi^{\mathrm{E}+}$ is the Eulerian gravitational-potential increment ϕ^{E} on the exterior side of ∂V and $\psi^{\mathrm{E}-}$ is the Eulerian centrifugal-potential increment ψ^{E} on the interior side of ∂V. Moreover, the continuity of the normal component of the displacement vector on ∂C, that is, $\vec{e}_{\mathrm{r}}\cdot\vec{u}(b^+)=\vec{e}_{\mathrm{r}}\cdot\vec{u}(b^-)$, has been applied in eq. (63). The boundary-value function $b_1^{\partial C}$ can be further rewritten in the form analogous to eq. (64)

$$b_1^{\partial C}=-\frac{1}{4\pi G}\left(\operatorname{grad}\phi^{\mathrm{E}-}\cdot\vec{e}_{\mathrm{r}}+\frac{2}{b}\psi^{\mathrm{E}-}\right)-\varrho_0^-(\vec{u}^+\cdot\vec{e}_{\mathrm{r}}). \tag{65}$$

In other words, defining $b_1^{\partial V}$ and $b_1^{\partial C}$ in the forms (64) and (65), respectively, guarantees that the boundary conditions for the Eulerian gravity increment on bounding surfaces ∂C and ∂V are satisfied.

5.3 Spherical harmonic parametrization

It has become convenient to use spherical coordinates (r, Ω), $\Omega = (\vartheta, \varphi)$ when dealing with the viscoelastic response of a spherical earth model and parametrize field variables in terms of surface spherical harmonics. Such a parametrization has been used, for instance, by Peltier (1974), Wu & Peltier (1982) and others. Here, we only introduce the representation form for the Eulerian gravitational-potential increment ϕ^{E} and refer to Martinec (2000, eqs 55–57) for the parametrizations of other field variables. For a fixed time and $b \le r \le a$, the angular dependence of ϕ^{E} is described as a series of scalar spherical harmonics $Y_{jm}(\Omega)$ (e.g. Varshalovich *et al.* 1989, chapter 5):

$$\phi^{\mathrm{E}}(r,\Omega)=\sum_{j=0}^{\infty}\sum_{m=-j}^{j}\phi_{jm}^{\mathrm{E}}(r)Y_{jm}(\Omega), \tag{66}$$

where $\phi_{jm}^{\mathrm{E}}(r)$ are the spherical harmonic expansion coefficients depending on the radial coordinate r. Note that the same parametrization as in eq. (66) is taken for the test function $\delta\phi^{\mathrm{E}}$. The spherical harmonic representation of eq. (37) then reads as

$$\Phi_{jm}^{\mathrm{E}}(r)=\phi_{jm}^{\mathrm{E}}(r)+\psi_{jm}^{\mathrm{E}}(r), \tag{67}$$

where $\Phi^{\mathrm{E}}_{jm}(r)$ and $\psi^{\mathrm{E}}_{jm}(r)$ are the spherical harmonic expansion coefficients of the Eulerian gravity-potential increment Φ^{E} and the Eulerian centrifugal-potential increment ψ^{E}, respectively. The later coefficients are given by the representation (30) where they are equal to zero unless $j = 0$, or $j = 2$ and $m = 0, \pm 1$.

We now aim at expressing the boundary-value functions $b_1^{\partial C}$ and $b_1^{\partial V}$ in spherical harmonic representation. Since the Eulerian density increment vanishes outside the Earth and in a fluid core (as discussed in Section 4.1), the Eulerian gravitational-potential increment is harmonics outside the solution domain B,

$$\nabla^2 \phi^{\mathrm{E}} = 0 \quad \text{outside } B. \tag{68}$$

Moreover, it passes continuously through the boundaries of B,

$$\left[\phi^{\mathrm{E}}\right]^{+}_{-} = 0 \quad \text{on } \partial C \cup \partial V. \tag{69}$$

The solution of this boundary-value problem with an additional requirement that ϕ^{E} is regular at the origin and vanishes at infinity is

$$\phi^{\mathrm{E}}(r, \Omega) = \begin{cases} \displaystyle\sum_{j=0}^{\infty} \sum_{m=-j}^{j} \left(\frac{a}{r}\right)^{j+1} \phi^{\mathrm{E}}_{jm}(a^-) Y_{jm}(\Omega) & \text{for } r \geq a, \\ \displaystyle\sum_{j=0}^{\infty} \sum_{m=-j}^{j} \left(\frac{r}{b}\right)^{j} \phi^{\mathrm{E}}_{jm}(b^+) Y_{jm}(\Omega) & \text{for } r \leq b. \end{cases} \tag{70}$$

Differentiating the last expression with respect to r and referring the results to the external sides of ∂B yields

$$\vec{e}_{\mathrm{r}} \cdot \operatorname{grad} \phi^{\mathrm{E}}(r, \Omega) = \begin{cases} \displaystyle\frac{1}{a} \sum_{j=0}^{\infty} \sum_{m=-j}^{j} (-j-1) \phi^{\mathrm{E}}_{jm}(a^-) Y_{jm}(\Omega) & \text{for } r = a^+, \\ \displaystyle\frac{1}{b} \sum_{j=0}^{\infty} \sum_{m=-j}^{j} j \phi^{\mathrm{E}}_{jm}(b^+) Y_{jm}(\Omega) & \text{for } r = b^-. \end{cases} \tag{71}$$

where the continuity of ϕ^{E} on ∂C and ∂V, that is eqs $(25)_1$ and $(26)_1$, have been used. Substituting for $\phi^{\mathrm{E}}_{jm}(a^-)$ and $\phi^{\mathrm{E}}_{jm}(b^+)$ from eq. (67) yields

$$\vec{e}_{\mathrm{r}} \cdot \operatorname{grad} \phi^{\mathrm{E}}(r, \Omega) = \begin{cases} \displaystyle\frac{1}{a} \sum_{j=0}^{\infty} \sum_{m=-j}^{j} \left[(-j-1)\Phi^{\mathrm{E}}_{jm}(a^-) + (j+1)\psi^{\mathrm{E}}_{jm}(a^-)\right] Y_{jm}(\Omega) & \text{for } r = a^+, \\ \displaystyle\frac{1}{b} \sum_{j=0}^{\infty} \sum_{m=-j}^{j} \left[j\Phi^{\mathrm{E}}_{jm}(b^+) - j\psi^{\mathrm{E}}_{jm}(b^+)\right] Y_{jm}(\Omega) & \text{for } r = b^-. \end{cases} \tag{72}$$

The boundary-value functions $b_1^{\partial V}$ and $b_1^{\partial C}$, expressed by eqs (64) and (65), respectively, can now be represented as

$$b_1^{\partial V} = \frac{1}{4\pi G a} \sum_{j=0}^{\infty} \sum_{m=-j}^{j} \left[(-j-1)\Phi^{\mathrm{E}}_{jm}(a^-) + (j+3)\psi^{\mathrm{E}}_{jm}(a^-)\right] Y_{jm}(\Omega) - \sigma^{\mathrm{L}}, \tag{73}$$

and

$$b_1^{\partial C} = \frac{1}{4\pi G b} \sum_{j=0}^{\infty} \sum_{m=-j}^{j} \left[j\Phi^{\mathrm{E}}_{jm}(b^+) + (-j+2)\psi^{\mathrm{E}}_{jm}(b^+)\right] Y_{jm}(\Omega) - \varrho_0^-(\vec{u}^+ \cdot \vec{e}_{\mathrm{r}}). \tag{74}$$

By comparing the boundary-value functions (73) and (74) with those for a non-rotating Earth (Martinec 2000, eq. 38) we can find that there are two additional boundary-value terms in eqs (73) and (74), that is

$$b_1^{\partial V,\psi} = \frac{1}{4\pi G a} \sum_{j=0}^{\infty} \sum_{m=-j}^{j} (j+3)\psi^{\mathrm{E}}_{jm}(a^-) Y_{jm}(\Omega), \tag{75}$$

and

$$b_1^{\partial C,\psi} = \frac{1}{4\pi G b} \sum_{j=0}^{\infty} \sum_{m=-j}^{j} (-j+2)\psi^{\mathrm{E}}_{jm}(b^+) Y_{jm}(\Omega), \tag{76}$$

which describe the feedback of the centrifugal-potential increment on the linear-momentum balance.

5.4 Numerical implementation of the rotational feedback

Fig. 1 illustrates the basic components for the description of the GIA-induced variations in the rotation vector and the associated feedback mechanics, that is, the rotationally induced variations in deformation and gravity. These components are the gravito-viscoelastic equations

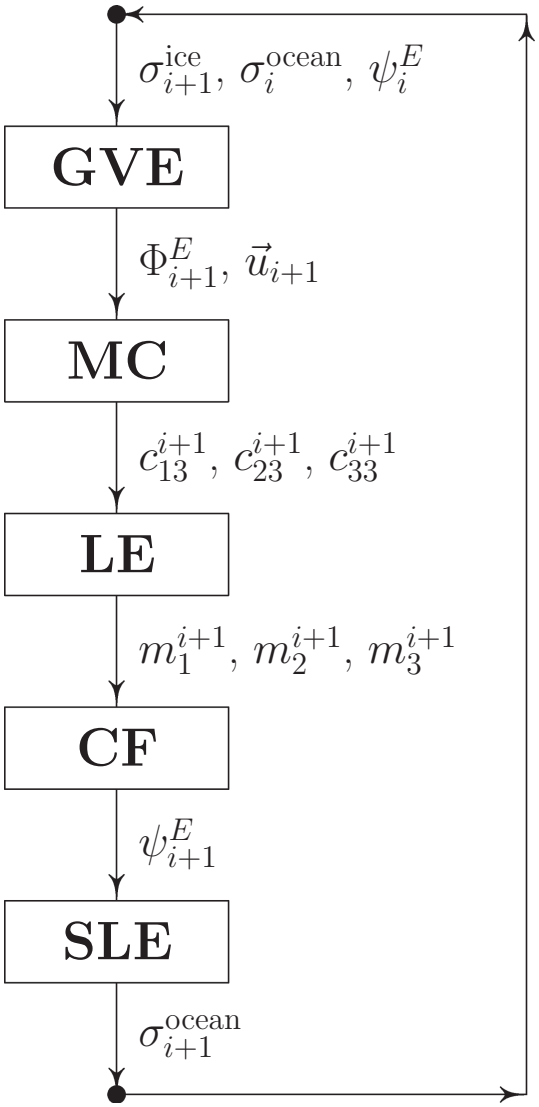

Figure 1. Schematic illustration of the implementation of the GIA-induced variations in the rotation parameters and the associated feedback mechanics of the rotationally induced variations in deformation and gravity between time epochs t_i and t_{i+1}. The numerical algorithm solves the first four steps in the spherical harmonic domain. Then, the output quantities are transformed into the spatial domain and the SLE is solved in the last step (see text for further details).

(GVE) governing the load-induced perturbation of the hydrostatic equilibrium reference configuration, MacCullagh's formula describing the variation of the inertia-tensor increment, the Liouville equation describing the motion of the rotation axes, the variation of the centrifugal force (CF) and the sea level equation (SLE) controlling the redistribution of water in the ice-ocean system. The evaluation of the coupled system of equations from time epoch t_i to time epoch t_{i+1} is implemented in the five-step algorithm. The arrows indicate the flow of the operations.

In the first step, the spatial and time varying ice-mass load $\sigma_{i+1}^{\text{ice}}$ over continents is prescribed as input data. The water-mass load σ_i^{ocean} over oceans and the Eulerian centrifugal-potential increment ψ_i^{E} are known from the previous time t_i solution. The total surface-mass load at the start of time epoch t_{i+1} is

$$\sigma_{i+1}^{\text{L}} = \sigma_{i+1}^{\text{ice}} + \sigma_i^{\text{ocean}}. \tag{77}$$

The GVEs describing the load-induced perturbation of a spherical, self-gravitating, incompressible, Maxwell-viscoelastic continuum, extended for the centrifugal-potential increment, as derived in Section 5.2, are solved by the spectral finite-element method developed by Martinec (2000). There, the radial dependence of the field variables is parametrized by finite elements, whereas the lateral dependence is parametrized by spherical harmonics. This method provides the displacement vector $\vec{u}$ and the Eulerian gravity-potential increment Φ^{E} at time t_{i+1}.

In the second step, the degree 0 and degree 2 spherical harmonic components of the gravitational-potential increment ϕ^{E} are computed by

$$\phi_{jm}^{\text{E}}(r, t_{i+1}) = \Phi_{jm}^{\text{E}}(r, t_{i+1}) - \psi_{jm}^{\text{E}}(r, t_i), \tag{78}$$

for $j = 0, 2$, $m = 0, 1$ and $b \le r \le a$. Here, the degree 0 and degree 2 spherical harmonic components of the centrifugal-potential increment ψ^{E} are expressed by eq. (30). The temporal perturbation of the inertia tensor, required to be specified in the Liouville equation, is then derived from time variations of the degree 2 spherical harmonic components of the gravitational-potential increment by MacCullagh's formulae (Martinec & Hagedoorn 2005, eqs 79 and 89),

$$c_{13}(t) = -\sqrt{\frac{5}{6\pi}}\frac{a^3}{G}\mathrm{Re}\left[\phi^{\mathrm{E}}_{21}(t)\right],$$

$$c_{23}(t) = \sqrt{\frac{5}{6\pi}}\frac{a^3}{G}\mathrm{Im}\left[\phi^{\mathrm{E}}_{21}(t)\right],$$

$$c_{33}(t) = \frac{1}{3}\sqrt{\frac{5}{\pi}}\frac{a^3}{G}\phi^{\mathrm{E}}_{20}(t) + \frac{1}{3}\mathrm{Tr}\,\boldsymbol{c}(t), \tag{79}$$

where Re and Im are the real and imaginary parts of a complex number, respectively, and $\mathrm{Tr}\,\boldsymbol{c}(t)$ is the trace of the inertia-tensor increment. Note that under the incompressibily condition $\mathrm{div}\,\vec{u} = 0$ and surface-mass conservation, that is when $\sigma^{\mathrm{L}}_{00}(t) = 0$ at any time t, the trace of $\boldsymbol{c}^{\mathrm{L}}(t)$ vanishes, $\mathrm{Tr}\,\boldsymbol{c}(t) = 0$.

In the third step, the motion of the rotation axis of the deformed Earth is governed by the Liouville equation. This step was studied in detail by (Martinec & Hagedoorn 2005, sections 2.5 and 2.6). We showed that the Chandler wobbling of the rotation vector can be removed by moving-average filtering of $m(t)$ over the Chandler-wobble period. As a result, the long-term motion of the rotation vector is governed by eqs (17) and (18). Assuming that there is no rigid-body rotation of the configuration $\kappa(t)$ with respect to the corotating frame $O(x_1, x_2, x_3)$, the relative angular-momentum vector vanishes, $\vec{h}(t) = 0$ for $t > 0$ (Martinec & Hagedoorn 2005, eq. 27), and eqs (17) and (18) reduce to

$$m_1(t) = \frac{c_{13}(t)}{C - A}, \quad m_2(t) = \frac{c_{23}(t)}{C - A}, \quad m_3(t) = -\frac{c_{33}(t)}{C}. \tag{80}$$

In the fourth step, the rotation parameters are substituted into eq. (30) and the centrifugal-potential increment ψ^{E} is updated for time epoch t_{i+1}. Finally, the spherical harmonics of the gravity-potential increment can be updated,

$$\Phi^{\mathrm{E}}_{jm}(r, t_{i+1}) = \phi^{\mathrm{E}}_{jm}(r, t_{i+1}) + \psi^{\mathrm{E}}_{jm}(r, t_{i+1}), \tag{81}$$

and transformed, together with the spherical harmonic representation of the displacement $\vec{u}(t_{i+1})$, into the spatial domain. The time epoch t_{i+1} ends with solving the sea level equation for $\sigma^{\mathrm{ocean}}_{i+1}$ following the implementation by Hagedoorn *et al.* (2007).

6 THE LOVE-NUMBER APPROACH FOR POLAR MOTION

The polar motion of the Earth's rotation axis as a response to surface-mass load variations during glaciation periods is traditionally computed in the LD using the method proposed by Sabadini *et al.* (1982). This method requires that not only the initial density $\varrho_0(r)$ but also the viscosity and elastic parameters vary only radially.

To model the polar motion of the rotation axis due to the motion inside the deforming Earth and the change of the gravitational and centrifugal forces, the inertia-tensor increment $c(t)$ in the polar-motion excitation function $\chi(t)$ consists of two contributions, $c^{\mathrm{L}}(t)$ and $c^{\mathrm{R}}(t)$, as shown in eq. (15), and the contribution $c^{\mathrm{CF}}(t)$ due to the centrifugal-potential increment ψ^{E},

$$c(t) = c^{\mathrm{L}}(t) + c^{\mathrm{R}}(t) + c^{\mathrm{CF}}(t), \tag{82}$$

where

$$c^{\mathrm{R}}(t) = k^{\mathrm{L}}(t) * c^{\mathrm{L}}(t), \tag{83}$$

$k^{\mathrm{L}}(t)$ is the second-degree loading Love number for the gravitational potential (e.g. Peltier 1974, 1976; Wu & Peltier 1982) and the asterisk * denotes the time convolution. Munk & MacDonald (1960, section 5.3) and Moritz & Mueller (1987, section 3.2) showed that

$$c^{\mathrm{CF}}(t) = (C - A)\frac{k^{\mathrm{T}}(t)}{k_{\mathrm{s}}} * m(t), \tag{84}$$

where $k^{\mathrm{T}}(t)$ is the second-degree tidal Love number for the gravitational potential and k_{s} is the secular Love number,

$$k_{\mathrm{s}} = 3G(C - A)/\Omega_0^2 a^5. \tag{85}$$

By eqs (82)–(84), the linearized Liouville equation (18) for polar motion becomes

$$\left[\delta(t) - \frac{k^{\mathrm{T}}(t)}{k_{\mathrm{s}}}\right] * m(t) = \chi^{\mathrm{L+R}}(t), \tag{86}$$

where $\delta(t)$ is the Dirac delta function and

$$\chi^{\mathrm{L+R}}(t) = \frac{1}{C - A}[\delta(t) + k^{\mathrm{L}}(t)] * c^{\mathrm{L}}(t). \tag{87}$$

Applying the Laplace transform to eq. (86) results in

$$m(s) = \mathcal{M}(s)\chi^{\mathrm{L+R}}(s), \tag{88}$$

where $m(s)$ is the Laplace image of $m(t)$,

$$\chi^{\mathrm{L+R}}(s) = \frac{1}{C-A}[1 + k^{\mathrm{L}}(s)]c^{\mathrm{L}}(s), \tag{89}$$

and

$$\mathcal{M}(s) = \frac{1}{1 - \dfrac{k^{\mathrm{T}}(s)}{k_{\mathrm{s}}}} \tag{90}$$

is the Laplace-transformed polar-motion transfer function representing the displacement of the rotation axis of the instantaneous configuration $\kappa(t)$ with respect to the co-rotating frame $O(x_1, x_2, x_3)$ for a unit surface-mass loading excitation (Spada *et al.* 2011).

The objective of this section is to compare the polar-motion function $m(t)$ calculated by the LD method with that resulting from the TD method (presented in Section 5). For this reason, we identify the secular Love number with the fluid tidal Love number

$$k_{\mathrm{s}} \equiv k_{\mathrm{f}}^{\mathrm{T}}. \tag{91}$$

This assumption means that the Earth has reached its rotational equilibrium prior to the application of the surface load. This assumption may, however, be violated due to (i) unrelaxed lithospheric stresses in the initial configuration of a viscoelastic earth model comprising an elastic lithosphere, (ii) lateral density variations in the Earth's mantle caused by thermal and compositional heterogeneities or (iii) non-zero deviatoric pre-stresses induced by convection currents in the mantle. Within the framework of traditional GIA theory, there is no rigorous mathematical tool to take these effects into account. Since $k_{\mathrm{f}}^{\mathrm{T}}$ differs very little from the observational value of k_{s}, Mitrovica *et al.* (2005) added a small correction (the so-called β-correction) to the fluid Love number to adjust the observed secular Love number. By this, elastic-lithosphere and mantle-convection effects are accounted for when modelling glacial-induced perturbations of the Earth's rotation.

In the case when the Chandler wobble is not included in $\mathcal{M}(s)$ and assumption (91) is adopted, eq. (88) can be arranged as (e.g. Wu & Peltier 1984; Vermeersen *et al.* 1997; Mitrovica & Milne 1998; Sabadini & Vermeersen 2004; Spada *et al.* 2011)

$$\mathcal{M}(s) = A_{\mathrm{e}} + \frac{A_{\mathrm{s}}}{s} + \sum_{i=1}^{M-1} \frac{A_i}{s - a_i}, \tag{92}$$

where a_i are the roots of a degree $M-1$ polynomial dispersion equation and represent the (real) rotational counterparts of the viscous gravitational relaxation frequencies s_i. Making use of the product identity (A2), the elastic A_{e}, secular A_{s} and viscous A_i rotational residues are expressed as

$$A_{\mathrm{e}} = \frac{\sigma_{\mathrm{r}}}{\sigma_0}, \quad A_{\mathrm{s}} = -\frac{\sigma_{\mathrm{r}}}{\sigma_0}\frac{\prod_{i=1}^{M} s_i}{\prod_{i=1}^{M-1} a_i}, \quad A_i = \frac{\sigma_{\mathrm{r}}}{\sigma_0}\frac{1}{a_i}\frac{\prod_{k=1}^{M}(s_k - a_i)}{\prod_{k\neq i}^{M-1}(a_k - a_i)}, \tag{93}$$

where σ_{r} is the Chandler-wobble angular frequency for a rigid earth,

$$\sigma_0 = \frac{k^{\mathrm{T}}(s=0) - k_{\mathrm{e}}^{\mathrm{T}}}{k^{\mathrm{T}}(s=0)}\,\sigma_{\mathrm{r}}, \tag{94}$$

and k_e^{T} is the elastic second-degree tidal Love number for the gravitational potential.

6.1 Numerical results for polar motion

We now compute the polar motion of the rotating, spherically symmetric, five-layer, incompressible, self-gravitating, viscoelastic earth model M3-L70-V01 (Spada *et al.* 2011, table 3) used in the benchmark study of numerical performance of GIA computational codes based on different mathematical and numerical approaches. The Green's functions of this model are computed analytically (e.g. Sabadini *et al.* 1982; Wu & Peltier 1984; Milne & Mitrovica 1996). The surface-mass load is represented by a spherical cap with surface-mass density $\sigma(\vartheta)$ centred at the colatitude $\vartheta_{\mathrm{c}} = 25^\circ$ and longitude $\lambda_{\mathrm{c}} = 75^\circ$. The parameters of the spherical-cap load are given by (Spada *et al.* 2011, table 4).

Let a spherical-cap load $\sigma(\vartheta)$ be centred at the north pole and σ_j be the expansion coefficients of $\sigma(\vartheta)$ into a series of Legendre polynomials $P_j(\cos\vartheta)$. The same load, but centred at colatitude ϑ_{c} and longitude λ_{c}, that is the load $\sigma(\vartheta, \lambda)$, is represented by the series of spherical harmonics in the form

$$\sigma(\vartheta, \lambda) = \sum_{j=0}^{\infty}\sum_{m=-j}^{j} \sigma_{jm} Y_{jm}(\vartheta, \lambda), \tag{95}$$

where the expansion coefficients σ_{jm} are related to σ_j by

$$\sigma_{jm} = \frac{4\pi}{2j+1}\,\sigma_j\,Y^*_{jm}(\vartheta_c, \lambda_c). \tag{96}$$

In particular, for $j = 2$ and $m = 1$, we have

$$\sigma_{21} = -\sqrt{\frac{3\pi}{10}}\,\sigma_2 \sin 2\vartheta_c\, e^{-i\lambda_c}. \tag{97}$$

A simple loading history is simulated by the Heaviside function $f(t) = H(t)$. The surface-mass load σ^L is then

$$\sigma^L = \sigma(\vartheta, \lambda) f(t). \tag{98}$$

The inertia-tensor increment $c^L(t)$ due to surface-mass load is

$$c^L(t) = (C - A) G_\sigma f(t), \tag{99}$$

where the geometrical factor G_σ is determined by the load geometry (Spada *et al.* 2011, eq. 31),

$$G_\sigma = \sqrt{\frac{8\pi}{15}}\,\frac{a^4}{C-A}\,\sigma^*_{21}. \tag{100}$$

Transforming eq. (99) to the LD and substituting the result into eq. (89) yields

$$\chi^{L+R}(s) = G_\sigma[1 + k^L(s)] f(s), \tag{101}$$

where $f(s)$ is the Laplace image of $f(t)$. The polar motion (eq. 88) which now includes a loading effect is

$$m(s) = G_\sigma[1 + k^L(s)]\mathcal{M}(s) f(s). \tag{102}$$

Substituting for $k^L(s)$ (e.g. Peltier 1976) for $\mathcal{M}(s)$ from eq. (92) (Vermeersen *et al.* 1994; Mitrovica & Milne 1998; Sabadini & Vermeersen 2004; Spada *et al.* 2011) showed that

$$m(s) = G_\sigma\left(A'_e + \frac{A'_s}{s} + \sum_{i=1}^{M-1}\frac{A'_i}{s - a_i}\right) f(s), \tag{103}$$

where the elastic A'_e, secular A'_s and viscous A'_i amplitudes are given by Spada *et al.* (2011, eqs 23–25). The other viscous amplitudes denoted by A''_i in Spada *et al.* (2011) are shown to vanish identically. For Heaviside loading ($f(s) = 1/s$), the inverse Laplace transform of eq. (103) results in

$$m(t) = G_\sigma\left[A'_e + A'_s t + \sum_{i=1}^{M-1}\frac{A'_i}{a_i}(e^{a_i t} - 1)\right] H(t). \tag{104}$$

Fig. 2 compares the x and y Cartesian components of the polar-motion function $m(t)$ computed by the TD method (solid lines) with those resulting from the LD method (dashed lines). The dashed and solid curves show excellent agreement for all chosen time instances, which means that the extended TD method for calculating $m(t)$ (presented in Section 5) is fully consistent with the traditional LD solution to $m(t)$.

It should be emphasized that the two methods are independent of each other and calculate the polar-motion function $m(t)$ in rather different ways. The extended TD method includes the effect of changes in the centrifugal force in the linear-momentum equation (41) which

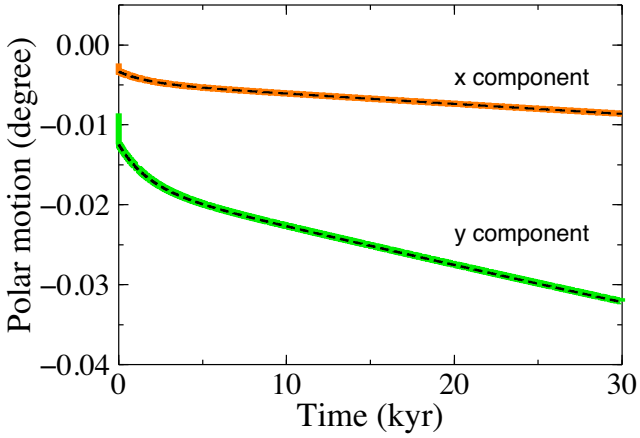

Figure 2. The x and y Cartesian components of the polar motion function $m(t)$ computed by the extended TD method (solid colour lines) and the traditional LD method (dashed lines). In all calculations, the results apply to the spherically symmetric, incompressible viscoelastic earth model M3-L70-V01 (Spada *et al.* 2011, table 3) loaded by a spherical cap (Spada *et al.* 2011, table 4) centred at the colatitude $\vartheta_c = 25^\circ$ and longitude $\lambda_c = 75^\circ$.

is coupled with the linearized Liouville equation (18) for determining the polar motion $m(t)$. It is important to emphasize that eq. (18) does not contain the contribution of the centrifugal-force change. The LD method does not consider the change of the centrifugal force in the linear-momentum equation (41), but it includes an additional term $c^{\rm CF}(t)$ in the linearized Liouville equation (86) for determining the polar motion $m(t)$. In this respect, the LD method considers the effect of the change of the centrifugal force on deformation and gravity to be negligible. In the following section, we aim to show that this approximation is not correct for the deformation and gravity field of degree $j = 2$ and order $m = 1$.

6.2 Rotational feedback on displacement and gravity

Having found the polar-motion function $m(t)$, the Eulerian centrifugal-potential increment $\psi^{\rm E}_{21}(t)$ is determined by eq. $(30)_2$. Substituting $\psi^{\rm E}_{21}$ into eqs (75) and (76), the degree 2 and order 1 spherical harmonic of the boundary-value functions $b_1^{\partial V,\psi}$ and $b_1^{\partial C,\psi}$ is

$$b^{\partial V,\psi}_{1,21} = G_\psi m^*,$$
$$b^{\partial C,\psi}_{1,21} = 0, \tag{105}$$

where

$$G_\psi = -\sqrt{\frac{5}{24\pi}}\,\frac{\Omega_0^2 a}{G}. \tag{106}$$

Hence, only the boundary-value function $b^{\partial V,\psi}_{1,21}(t)$ describes the feedback of the polar motion $m(t)$ on displacement and gravity.

The solution of the initial, boundary-value problem (51) with the boundary conditions (73) and (74) for degree $j = 2$ and order $m = 1$, that is function $Y_{21}(r, t)$, where Y_{21} stands for the vertical and horizontal amplitudes of the displacement, U_{21} and V_{21}, respectively, and for the amplitudes of the gravity potential, $\Phi^{\rm E}_{21}$. It is composed of two parts,

$$Y_{21}(r, t) = Y^{\rm L}_{21}(r, t) - Y^{\psi}_{21}(r, t), \tag{107}$$

where the first part, $Y^{\rm L}_{21}(r, t)$, expresses the response of the viscoelastic earth model to surface-mass load variations $\sigma^{\rm L}(t)$, while the second part, $Y^{\psi}_{21}(r, t)$, expresses the response of the viscoelastic earth model to polar-motion variations $m(t)$. The opposite signs on the right-hand side of eq. (107) account for the opposite signs at $b_1^{\partial V,\psi}$ and $\sigma^{\rm L}$ in the boundary condition (73).

The first part is commonly included in computations of the viscoelastic response functions $Y_{21}(r, t)$. For the surface-mass load $\sigma^{\rm L}(t)$ in the form of spherical harmonic series (95) and the Heaviside loading, it holds that (e.g. Peltier 1974, 1976; Wu & Peltier 1982)

$$Y^{\rm L}_{21}(r, t) = \sigma_{21}\left[y^{\rm L}_{\rm e} + \sum_{k=1}^{M} \frac{y^{\rm L}_k}{s_k}(\mathrm{e}^{s_k t} - 1)\right]H(t), \tag{108}$$

where the symbol $y^{\rm L}$ stands for the viscoelastic load Love numbers $h^{\rm L}$, $\ell^{\rm L}$ and $k^{\rm L}$ for the vertical and horizontal displacements and the incremental gravitational potential, respectively. The elastic amplitudes $y^{\rm L}_{\rm e}$ and viscous amplitudes $y^{\rm L}_k$ depend on the radial distance r from the centre of the sphere, hence $Y^{\rm L}_{21}$. The loading Love numbers $y^{\rm L}$ and the viscous gravitational relaxation frequencies s_k are characterized by the harmonic degree j of a surface load, which is $j = 2$ in this particular case and is assumed to be implicit in eq. (108). Moreover, making use of eqs (85), (100) and (106) gives

$$\sigma_{21} = -k_{\rm s} G^*_\sigma G_\psi, \tag{109}$$

and $Y^{\rm L}_{21}(r, t)$ can be expressed in a more convenient form

$$Y^{\rm L}_{21}(r, t) = -k_{\rm s} G^*_\sigma G_\psi \left[y^{\rm L}_{\rm e} + \sum_{k=1}^{M} \frac{y^{\rm L}_k}{s_k}(\mathrm{e}^{s_k t} - 1)\right]H(t). \tag{110}$$

The second part, Y^{ψ}_{21}, has not yet been considered in computation of the viscoelastic response functions $Y_{21}(r, t)$. This part can be viewed as the rotational feedback of polar-motion variations to deformation and gravity potential. This part can be expressed as the time convolution of the second-degree tidal Love numbers $y^{\rm T}(r, t)$ with the boundary-value function $b_1^{\partial V,\psi}$,

$$Y^{\psi}_{21}(r, t) = y^{\rm T}(r, t) * b_1^{\partial V,\psi}(t), \tag{111}$$

or, in view of eq. (105),

$$Y^{\psi}_{21}(r, t) = G_\psi\, y^{\rm T}(r, t) * m^*(t). \tag{112}$$

Similarly to $y^{\rm L}$, the symbol $y^{\rm T}$ stands for the tidal Love numbers $h^{\rm T}$, $\ell^{\rm T}$ and $k^{\rm T}$ for the vertical and horizontal displacements and the incremental gravitational potential, respectively. The tidal Love numbers $y^{\rm T}$ are characterized by the harmonic degree j of tidal loading, which is $j = 2$ in this particular case, and is assumed to be implicit in eq. (112). Applying the Laplace transform to eq. (112) gives

$$Y^{\psi}_{21}(r, s) = G_\psi\, y^{\rm T}(r, s) m^*(s). \tag{113}$$

Substituting for the Laplace-transformed tidal Love numbers (e.g. Spada *et al.* 2011), and for $m(s)$ from eq. (103), we have

$$Y_{21}^{\psi}(r,s) = G_{\sigma}^{*} G_{\psi}\left(y_{\mathrm{e}}^{\mathrm{T}} - \sum_{k=1}^{M} \frac{y_{k}^{\mathrm{T}}}{s - s_{k}}\right)\left(A_{\mathrm{e}}' + \frac{A_{\mathrm{s}}'}{s} + \sum_{i=1}^{M-1} \frac{A_{i}'}{s - a_{i}}\right) f(s). \tag{114}$$

Making use of the product identity (A1 in Appendix A), we obtain

$$Y_{21}^{\psi}(r,s) = G_{\sigma}^{*} G_{\psi}\left(B_{\mathrm{e}} + \frac{B_{\mathrm{s}}}{s} + \sum_{i=1}^{M-1} \frac{B_{i}'}{s - a_{i}} + \sum_{i=1}^{M} \frac{B_{i}''}{s - s_{i}}\right) f(s), \tag{115}$$

where the elastic B_{e}, secular B_{s} and viscous B_{i}' and B_{i}'' residues are expressed as

$$B_{\mathrm{e}} = y_{\mathrm{e}}^{\mathrm{T}} A_{\mathrm{e}}', \tag{116}$$

$$B_{\mathrm{s}} = y_{\mathrm{f}}^{\mathrm{T}} A_{\mathrm{s}}', \tag{117}$$

$$B_{i}' = \left(y_{\mathrm{e}}^{\mathrm{T}} + \sum_{k=1}^{M} \frac{y_{k}^{\mathrm{T}}}{a_{i} - s_{k}}\right) A_{i}', \qquad i = 1, \ldots, M-1, \tag{118}$$

$$B_{i}'' = \left(A_{\mathrm{e}}' + \frac{A_{\mathrm{s}}'}{s_{i}} - \sum_{k=1}^{M-1} \frac{A_{k}'}{a_{k} - s_{i}}\right) y_{i}^{\mathrm{T}}, \qquad i = 1, \ldots, M, \tag{119}$$

and y_{f}^{T} is the tidal fluid Love number (e.g. Spada *et al.* 2011, eq. 2). For Heaviside loading [$f(s) = 1/s$], the inverse Laplace transform of eq. (115) results in

$$Y_{21}^{\psi}(r,t) = G_{\sigma}^{*} G_{\psi}\left[B_{\mathrm{e}} + B_{\mathrm{s}} t + \sum_{i=1}^{M-1} \frac{B_{i}'}{a_{i}}(\mathrm{e}^{a_{i} t} - 1) + \sum_{i=1}^{M} \frac{B_{i}''}{s_{i}}(\mathrm{e}^{s_{i} t} - 1)\right] H(t). \tag{120}$$

Substituting eqs (110) and (120) into (107), the complete relaxation of $Y_{21}(t)$ due to surface loading σ^{L} and the rotational feedback by polar motion $m(t)$ is

$$Y_{21}(r,t) = -G_{\sigma}^{*} G_{\psi}\left\{k_{\mathrm{s}}\left[y_{\mathrm{e}}^{\mathrm{L}} + \sum_{i=1}^{M} \frac{y_{i}^{\mathrm{L}}}{s_{i}}(\mathrm{e}^{s_{i} t} - 1)\right] + B_{\mathrm{e}} + B_{\mathrm{s}} t + \sum_{i=1}^{M-1} \frac{B_{i}'}{a_{i}}(\mathrm{e}^{a_{i} t} - 1) + \sum_{i=1}^{M} \frac{B_{i}''}{s_{i}}(\mathrm{e}^{s_{i} t} - 1)\right\} H(t). \tag{121}$$

Under assumption (91), our calculations show that

$$k_{\mathrm{s}} y_{i}^{\mathrm{L}} = -B_{i}'' \tag{122}$$

for any $i = 1, \ldots, M$. Then, eq. (121) is reduced to the form

$$Y_{21}(r,t) = -G_{\sigma}^{*} G_{\psi}\left\{k_{\mathrm{s}} y_{\mathrm{e}}^{\mathrm{L}} + B_{\mathrm{e}} + B_{\mathrm{s}} t + \sum_{i=1}^{M-1} \frac{B_{i}'}{a_{i}}(\mathrm{e}^{a_{i} t} - 1)\right\} H(t). \tag{123}$$

Comparing eqs (104) and (123), we can see that there is an important similarity in the time relaxation of the polar-motion function $m(t)$ and the relaxation of the deformation and gravity field $Y_{21}(t)$. Under assumption (91), Vermeersen *et al.* (1994), Sabadini & Vermeersen (2004) and Spada *et al.* (2011) showed that the time relaxation of the polar motion $m(t)$ is characterized only by the rotational frequencies a_{i}. This fact is expressed by eq. (104), where the amplitudes A_{i}'' of the relaxation modes characterized by the viscous gravitational relaxation frequencies s_{i} are equal to zero. Similarly, the time relaxation of the deformation and gravity field $Y_{21}(t)$ due to rotational feedback is characterized only by the rotational frequencies a_{i}. This fact is expressed by eq. (123), where the amplitudes B_{i}'' of the relaxation modes proceed by the viscous gravitational relaxation frequencies s_{i} are cancelled by the contribution $Y_{21}^{\mathrm{L}}(r,t)$ due to eq. (122).

Fig. 3 shows the time evolution of the spherical harmonic $U_{21}(r,t)$ of the vertical displacement and $F_{21}(r,t)$ of the gravity-potential perturbation at the surface of the sphere ($r = a$) after the onset of a spherical-cap load at $t = 0$. The TD solution (solid colour lines), defined by eq. (51) with the boundary conditions (73) and (74), is compared with the LD solution given by eq. (123) (dashed lines). We can see that there is again excellent agreement between the two solutions, despite being based on different mathematical and numerical approaches.

To demonstrate the importance of the rotational feedback for the deformation and gravity field on a rotating sphere, the displacement $U_{21}^{\mathrm{L}}(a,t)$ and gravitational potential $F_{21}^{\mathrm{L}}(a,t)$, which correspond to the solution with a surface loading only, are also shown in Fig. 3 (thin solid colour lines). We can see that the difference between the complete solution $U_{21}(r,t)$ and $F_{21}(r,t)$, which includes the rotational-feedback contributions $U_{21}^{\psi}(r,t)$ and $F_{21}^{\psi}(r,t)$, and the responses $U_{21}^{\mathrm{L}}(a,t)$ and $F_{21}^{\mathrm{L}}(a,t)$ to a surface loading only is significant, even immediately after the loading of the sphere by a surface load. We can conclude that the rotational feedback on the deformation and gravity fields U_{21} and F_{21} due to change in the centrifugal force is positive in the sense that it adds significant contributions to these fields.

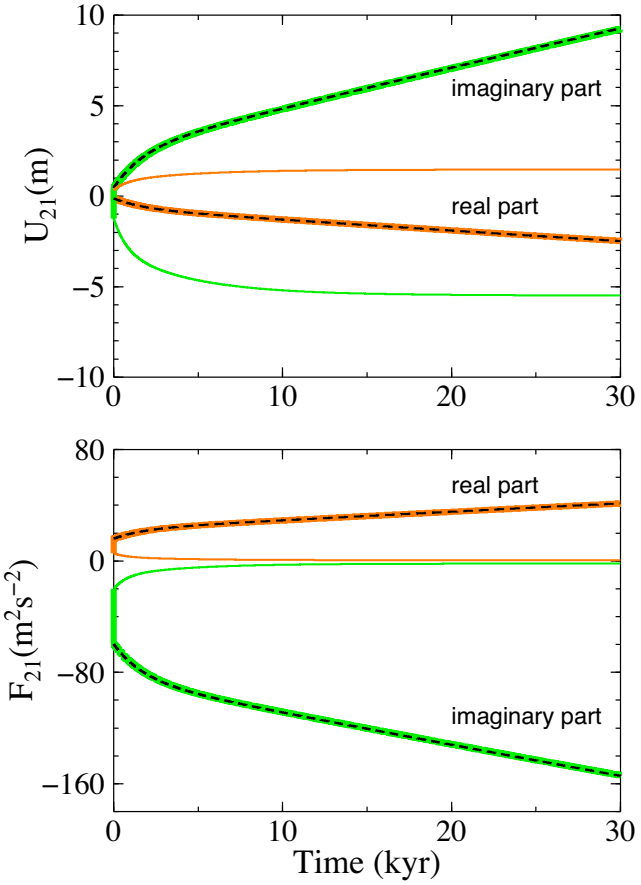

Figure 3. The spherical harmonic $U_{21}(t)$ of vertical displacement and $F_{21}(t)$ of gravity-potential perturbation at the surface of the sphere ($r = a$) computed by the extended TD method (thick solid colour lines, red = real part, green = imaginary part) and the extended LD method (dashed lines). These complete responses are compared with the responses $U^{\mathrm{L}}_{21}(t)$ and $F^{\mathrm{L}}_{21}(t)$ (thin solid colour lines) that are induced by surface loading only. The differences between the thick and thin lines are due to the rotational feedback of polar motion on vertical displacement and gravity-potential perturbation, that is $U^{\psi}_{21}(r, t)$ and $F^{\psi}_{21}(r, t)$.

To estimate the magnitude of the rotational feedback on linear-momentum balance, we calculate the GIA-induced radial displacement and sea level change since the Last Glacial Maximum (LGM) for the case where the rotational feedback is considered in linear-momentum balance, and compare it with the case where this feedback is not implemented. We again employ the rotating, spherically symmetric, five-layer, incompressible, self-gravitating, viscoelastic earth model M3-L70-V01 (Spada *et al.* 2011, table 3). The ice load is represented by the global ICE-3G deglaciation history proposed by Tushingham & Peltier (1992), which consists of 18 global ice-thickness distributions representing the deglaciation history from the LGM at 21 ka BP (before present) until today. We extend this model by a glaciation history starting at 120 ka BP according to Hagedoorn *et al.* (2007). While we acknowledge that this is not the most recent global ice model, the point of this discussion is to investigate the effect of the inclusion/exclusion of the rotational feedback. The ocean load is governed by the sea level equation that is implemented as described by Hagedoorn *et al.* (2007). We consider all feedbacks on the ocean load, that is, the effects of moving coast lines, grounded and floating ice and the centrifugal-potential increment due to the change in the Earth's rotation dynamics.

The top panel of Fig. 4 shows the surface distribution of radial displacement since the LGM for the case where the rotational feedback is implemented in the linear-momentum balance. This figure shows that the radial displacement reaches its largest values in the northern (up to 500 m) and southern (up to 200 m) polar regions due to the melting of the Fennoscandian, Laurentide and Antarctic ice sheets. The radial displacement has negative values of several tens of metres over the oceans (up to −45 m in the southern Indian ocean) due to increasing amount of melted water. The bottom panel of Fig. 4 shows the differences in radial displacement since the LGM between the cases with and without the rotational feedback included in the linear-momentum balance. We can see that the difference has the pattern of the degree 2 and order 1 spherical harmonic function. The differences result in modified surface deformation patterns with values reaching ±25 m, that is up to 10 per cent, in the areas of former or ongoing glaciations, but with significantly large changes in the deformation pattern in the ocean regions. For example, implementing or neglecting the rotational feedback in the linear-momentum balance affects the radial displacement of the bottom of the southern Indian ocean up to 50 per cent.

Furthermore, the top panel of Fig. 5 shows the spatial distribution of sea level change (i.e. the change in water-column load) since the LGM for the case where the rotational feedback is considered in the linear-momentum balance. The sea level overall is seen to have risen by about a 100 m over the open ocean (the equivalent sea level is 108 m). The bottom panel of Fig. 5 shows the differences in sea level change

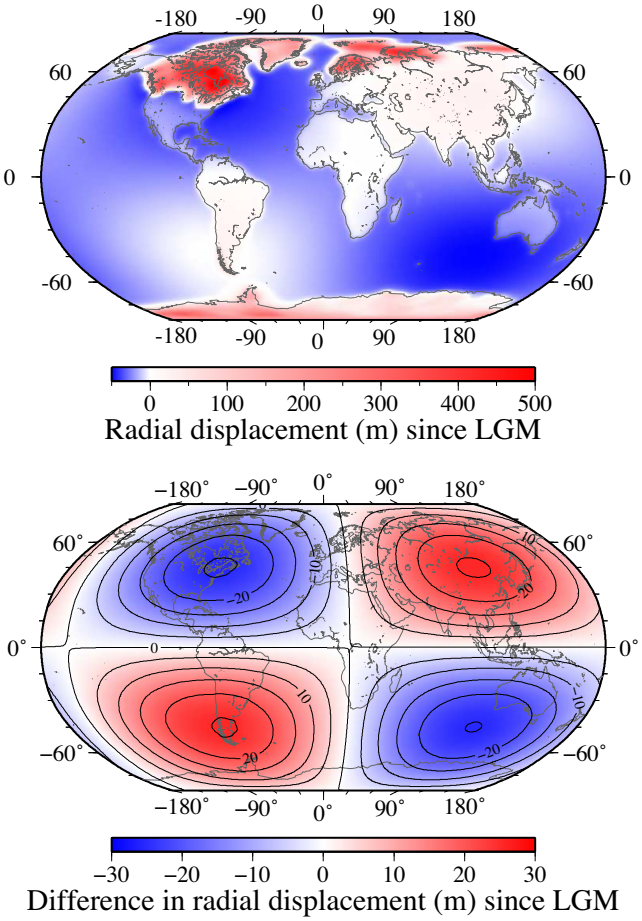

Figure 4. Top panel: The surface distribution of radial displacement since the LGM at 21 ka BP for the case where the rotational feedback is taken into account in the linear-momentum balance. Bottom panel: The difference in radial displacement since the LGM between the cases with and without the rotational feedback on linear-momentum balance. The results apply to the spherically symmetric, five-layer, incompressible, self-gravitating, viscoelastic earth model M3-L70-V01 (Spada *et al.* 2011) and the ICE-3G deglaciation model (Tushingham & Peltier 1992).

since the LGM between the cases where the rotational feedback is and is not implemented in the linear-momentum balance. As with the radial displacement, we can see that the difference has the pattern of the degree 2 and order 1 spherical harmonic function and reaches values of ± 1.8 m. The areas with different load histories with respect to moving coastlines are seen to be, for example, in the vicinity of Hudson Bay and along the Chinese, Australian and Argentinian coastlines. We can conclude from Figs 4 and 5 the importance of the rotational feedback on the linear-momentum balance.

6.3 Numerical results for the length of day (LOD)

For the sake of completeness, we compute the variations of the LOD induced by the GIA process. The LOD variations are dealt with (e.g. Munk & MacDonald 1960; Moritz & Mueller 1987; Sabadini & Vermeersen 2004)

$$\frac{\Delta \mathrm{LOD}}{\mathrm{LOD}}(t) = \frac{c_{33}(t)}{C}, \tag{124}$$

where LOD is a reference value of the length of day and c_{33} is the axial inertia-tensor increment in response to surface-mass redistribution and the associated viscoelastic response of the Earth.

The extended TD method computes the time-varying increment $c_{33}(t)$ by eq. $(79)_3$, after determining the degree 2 and order 0 spherical harmonic component of the gravitational-potential increment ϕ^{E} by eq. (78). Since the deformation of the Earth in response to ψ_{20} is included in the TD calculations, the spherical harmonic component ϕ^{E}_{20} is influenced by the time variation of ψ_{20}. This means that the extended TD method considers the bidirectional coupling between deformation and gravity on one side, and both the polar-motion and LOD variations on the other.

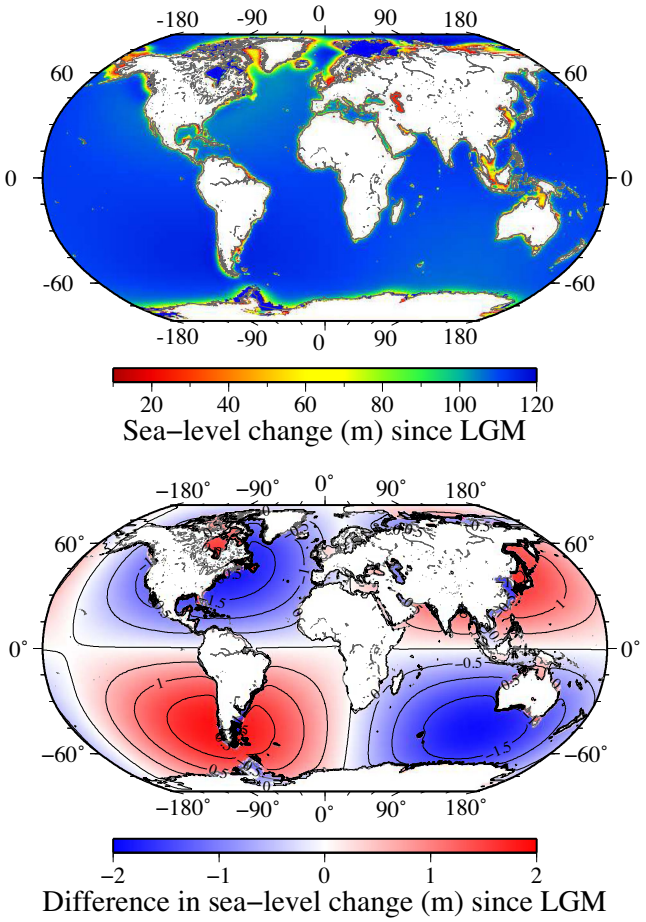

Figure 5. The same as Fig. 4, but for the sea level change.

To model the LOD variation due to the motion inside the deforming Earth and the change in the gravitational and centrifugal forces by the LD method, the inertia-tensor increment $c_{33}(t)$ in the LOD excitation function $\chi_3(t)$ consists of two contributions, $c^{L}_{33}(t)$ and $c^{R}_{33}(t)$, as shown in eq. (15), and the contribution $c^{CF}_{33}(t)$ due to the centrifugal-potential increment ψ^{E},

$$c_{33}(t) = c^{L}_{33}(t) + c^{R}_{33}(t) + c^{CF}_{33}(t), \tag{125}$$

where

$$c^{R}_{33}(t) = k^{L}(t) * c^{L}_{33}(t). \tag{126}$$

Munk & MacDonald (1960, section 5.3) showed that

$$c^{CF}_{33}(t) = -\frac{2}{3}(C - A)\frac{k^{T}(t)}{k_s} * m_3(t), \tag{127}$$

where the secular Love number k_s is given by eq. (85). However, Wu & Peltier (1984) and Spada (2003) consider the magnitude of c^{CF}_{33} being small in comparison to the magnitudes of c^{L}_{33} and c^{R}_{33}, and neglect c^{CF}_{33} in the total inertia-tensor increment c_{33}. Under this assumption, eqs (125) and (126) can be combined to give

$$c_{33}(t) = \left[\delta(t) + k^{L}(t)\right] * c^{L}_{33}(t). \tag{128}$$

The numerical example of the LOD variations will be presented for the earth model M3-L70-V01 (Spada *et al.* 2011, table 3), which is loaded by a spherical cap (Spada *et al.* 2011, table 4) centred at colatitude ϑ_c and longitude λ_c. For this load, the inertia-tensor increment c^{L}_{33} is (Spada *et al.* 2011, eq. 33)

$$c^{L}_{33} = \frac{4\pi}{15} a^4 \sigma_2 (3\cos^2\vartheta_c - 1). \tag{129}$$

Fig. 6 compares the LOD variations computed by the TD method (solid lines) with those resulting from the LD method (dashed lines). The dashed and solid curves show excellent agreement for all chosen time instances, which means that the methods are numerically consistent for calculating ΔLOD. Since the effect of the centrifugal-potential increment ψ^{E}_{20} on ΔLOD is only considered in the TD method, while the

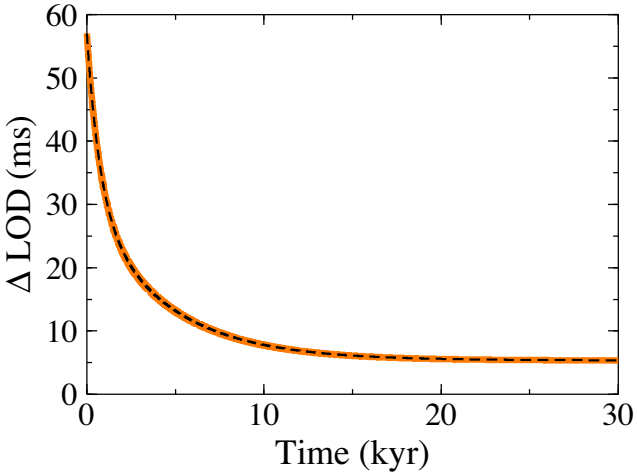

Figure 6. The LOD variation computed by the extended TD method (red line) and the traditional LD method (dashed line). The incremental centrifugal potential ψ_{20}^{E} is included only in the TD method, while the inertia-tensor increment c_{33}^{CF} is neglected in the LD solution.

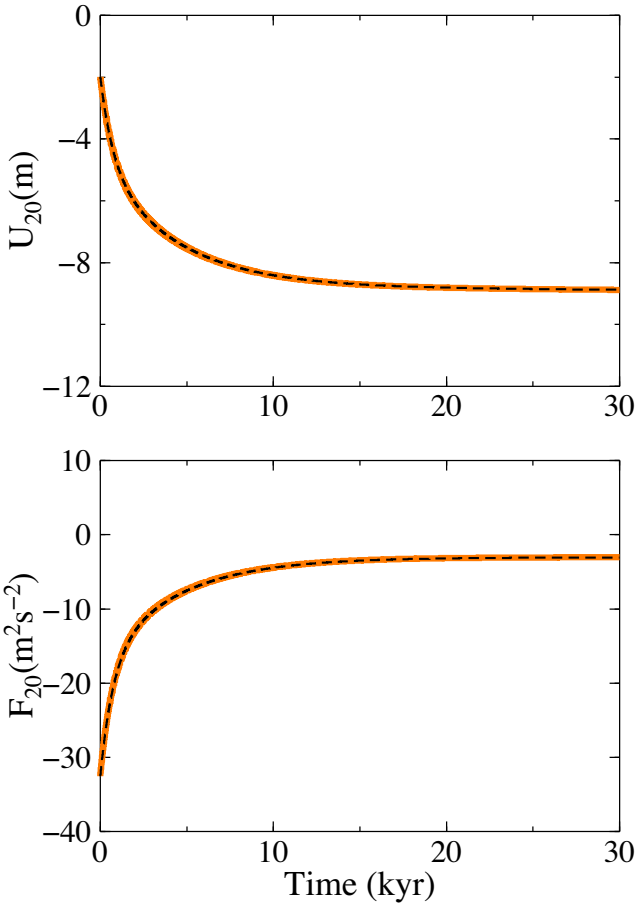

Figure 7. The spherical harmonic $U_{20}(t)$ of vertical displacement and $F_{20}(t)$ of gravity-potential perturbation at the surface of the sphere ($r = a$) computed by the extended TD method (red lines) and the traditional LD method (dashed lines). The incremental centrifugal force is included only in the TD method.

term c_{33}^{CF} is neglected in the LD solution, the numerical agreement between the two solutions shows that the effect of the centrifugal-potential increment ψ_{20}^{E} on ΔLOD is negligible, in agreement with Wu & Peltier (1984) and Spada (2003).

Fig. 7 shows the evolution of the spherical harmonic $U_{20}(r, t)$ of the vertical displacement and $F_{20}(r, t)$ of the gravity-potential perturbation at the surface of the sphere ($r = a$) after the onset of a spherical-cap load at $t = 0$. The TD solution (solid colour lines), defined by eq. (51) with the boundary conditions (73) and (74), is compared with the traditional LD solution based on the loading Love numbers (dashed lines). We can see that there is excellent agreement between the two solutions, although the former includes the rotational feedback of ΔLOD on

deformation and gravity while the latter neglects this effect. We can conclude that the rotational feedback of ΔLOD on the deformation and gravity fields U_{20} and F_{20} is small and can safely be neglected.

7 CONCLUSIONS

This paper has been motivated by an effort to extend the existing TD method (Martinec 2000) for modelling the GIA response of laterally heterogeneous earth models to include the effect of variations in the Earth's rotational dynamics. This was achieved by adding the perturbation in the centrifugal force into the linear-momentum equation and Poisson's equation and by coupling them with the linearized Liouville equation. Such a modification describes not only the direct effect, that is the change of the Earth's rotational dynamics in response to surface loading and the mass movement inside the Earth, but also the opposite effect, that is the change of deformation and gravity fields in response to varying rotational dynamics. We refer to the latter effect as the rotational feedback on the linear-momentum balance. We emphasize that this effect differs from the rotational feedback on the sea level equation where the incremental centrifugal potential is added to sea level equation. We do not deal with this effect in this paper, since it has already been studied intensively in literature (e.g. Milne & Mitrovica 1996; Peltier 1998).

After the mathematical extension of the TD method for the incremental centrifugal force and reaching numerical agreement on the polar-motion function against the LD method (Wu & Peltier 1984), another question arises involving how the degree 2 and order 1 spherical components of vertical displacement and incremental gravity potential computed by the extended TD method significantly differ from those computed by the LD method. It appears that the traditional LD method must also be extended to the rotational feedback on displacement and the gravity field. The extension is presented in Section and checked numerically against the extended TD method. Only after the extension of both of these methods for rotational effect, they provide consistent numerical results.

The extension of the LD method brings a new physical insight into the viscoelastic relaxation process on a rotating Earth. We show that the degree 2 and order 1 spherical components of vertical deformation and incremental gravity potential, that is U_{21} and F_{21}, relax in time with different relaxation frequencies than the other spherical harmonic components of deformation and gravity field. That is, the relaxation of U_{21} and F_{21} proceeds at the rotational frequencies, while the relaxation of the other spherical components does so by viscous gravitational relaxation frequencies. We show that the difference between the case where U_{21} and F_{21} relax in time with the rotational frequencies and where the relaxation is by viscous gravitational relaxation frequencies is significant. Since the later case corresponds to the traditional LD approach, we conclude that the extended LD method needs to be applied when computing the relaxation of the degree 2 and order 1 spherical components of vertical deformation and incremental gravity potential.

As far the variations in the LOD are concerned, the comparison between the extended TD method and the traditional LD method shows the LOD to be influenced by the variation of the centrifugal force only by a tiny amount, and this effect can be neglected. The feedback mechanism where the LOD variations influence the degree 2 and order 0 spherical harmonic components of deformation and gravity is also very small and can likewise be neglected.

ACKNOWLEDGEMENTS

The authors would like to thank Kevin Fleming and three anonymous reviewers for their comments on the manuscript that have helped to improve the manuscript. This work has been carried out within the framework of the research programme 11/RFP.1/GEO/3309 financed by the Science Foundation of Ireland. ZM acknowledges this support.

REFERENCES

Chambers, D.P., Wahr, J., Tamisiea, M.E. & Nerem, R.S., 2010. Ocean mass from GRACE and adjustment, *J. geophys. Res.,* **115,** B11415, doi:10.1029/2010JB007530.

Chambers, D.P., Wahr, J., Tamisiea, M.E. & Nerem, R.S., 2012. Reply to comment by W.R. Peltier *et al.* on 'Ocean mass from GRACE and glacial isostatic adjustment', *J. geophys. Res.,* **117,** B11404, doi:10.1029/2012JB009441.

Chinnery, M.A., 1975. The static deformation of an Earth with a fluid core: a physical approach, *Geophys. J. R. astr. Soc.,* **42,** 461–475.

Crossley, D.J. & Gubbins, D., 1975. Static deformation of the Earth's liquid core, *Geophys. Res. Lett.,* **2,** 1–4.

Dahlen, F.A., 1974. On the static deformation of an earth model with a fluid core, *Geophys. J. R. astr. Soc.,* **36,** 461–485.

Dahlen, F.A. & Tromp, J., 1998. *Theoretical Global Seismology,* Princeton Univ. Press.

Dziewonski, A.M. & Anderson, D.L., 1981. Preliminary reference earth model, *Phys. Earth planet. Inter.,* **25,** 297–356.

Farrell, W.E., 1972. Deformation of the Earth by surface loads, *Rev. Geophys. Space Phys.,* **10,** 761–797.

Hagedoorn, J.M., Wolf, D. & Martinec, Z., 2007. An estimate of global sea-level rise inferred from tide-gauge measurements using glacial isostatic models consistent with the relative sea-level record, *Pure appl. Geophys.,* **164,** 791–818.

Han, D. & Wahr, J., 1989. Post-glacial rebound analysis for a rotating Earth, in *Slow Deformations and Transmission of Stress in the Earth,* Vol. **49**, pp. 1–6, eds Cohen, S. & Vanicek, P., AGU Monograph Series.

Longman, I.M., 1963. A Green's function for determining the deformation of the Earth under surface mass loads 2: computations and numerical results, *J. geophys. Res.,* **68,** 485–496.

Martinec, Z., 2000. Spectral–finite element approach to three-dimensional viscoelastic relaxation in a spherical Earth, *Geophys. J. Int.,* **142,** 117–141.

Martinec, Z. & Hagedoorn, J., 2005. Time-domain approach to linearized rotational response of a three-dimensional viscoelastic earth model induced by glacial isostatic adjustment: I. Inertia-tensor perturbations, *Geophys. J. Int.,* **163,** 443–462.

Métivier, L., Collilieux, X. & Altamimi, Z., 2012. ITRF2008 contribution to glacial isostatic adjustment and recent ice melting assessment, *Geophys. Res. Lett.,* **39,** L01309, doi:10.1029/2011GL049942.

Milne, G.A. & Mitrovica, J.X., 1996. Postglacial sea-level change on a rotating Earth: first results from a gravitationally self-consistent sea-level equation, *Geophys. J. Int.,* **126,** F13–F20.
Milne, G.A. & Mitrovica, J.X., 1998. Postglacial sea-level change on a rotating Earth, *Geophys. J. Int.,* **133,** 1–19.
Mitrovica, J.X. & Milne, G.A., 1998. Glaciation-induced perturbations in the Earth's rotation: a new appraisal, *J. geophys. Res.,* **103,** 985–1005.
Mitrovica, J.X. & Wahr, J., 2011. Ice-age Earth rotation, *Ann. Rev. Earth planet. Sci.,* **39,** 577–616.
Mitrovica, J.X., Milne, G.A. & Davis, J.L., 2001. Glacial isostatic adjustment on a rotating Earth, *Geophys. J. Int.,* **147,** 562–578.
Mitrovica, J.X., Wahr, J., Matsuyama, I. & Paulson, A., 2005. The rotational stability of an ice-age Earth, *Geophys. J. Int.,* **161,** 491–506.
Moritz, H. & Mueller, I., 1987. *Earth Rotation, Theory and Observation,* Ungar Publishing Co.
Munk, W.H. & MacDonald, G. J.F., 1960. *The Rotation of the Earth: A Geophysical Discussion,* Cambridge Univ. Press.
Peltier, W.R., 1974. The impulse response of a Maxwell Earth, *Rev. Geophys.,* **12,** 649–669.
Peltier, W.R., 1976. Glacial isostatic adjustment, II: the inverse problem, *Geophys. J. R. astr. Soc.,* **46,** 669–706.
Peltier, W.R., 1998. Postglacial variations in the level of the sea: implications for climate dynamics and solid–Earth geophysics, *Rev. Geophys.,* **36,** 603–689.
Peltier, W.R., 1999. Global sea level rise and glacial isostatic adjustment, *Global planet. Change,* **20,** 93–123.
Peltier, W.R. & Drummond, R., 2010. Deepest mantle viscosity: constraints from Earth rotation anomalies, *Geophys. Res. Lett.,* **37,** L12304, doi:10.1029/2010GL043219.
Peltier, W.R. & Luthcke, S.B., 2009. On the origins of Earth rotation anomalies: new insights on the basis of both paleogeodetic data and Gravity Recovery and Climate Experiment (GRACE) data, *J. geophys. Res.,* **114,** B11405, doi:10.1029/2009JB006352.
Peltier, W.R., Drummond, R. & Roy, K., 2012. Comment on 'Ocean mass from GRACE and glacial isostatic adjustment' by Chambers, D.P. *et al.*, *J. geophys. Res.,* **117,** B11403, doi:10.1029/2011JB008967.
Roy, K. & Peltier, W.R., 2011. GRACE era secular trends in Earth rotation parameters: a global scale impact of the global warming process? *Geophys. Res. Lett.,* **38,** L10306, doi:10.1029/2011GL047282.
Sabadini, R. & Vermeersen, B., 2004. *Global Dynamics of the Earth. Applications of Normal Mode Relaxation Theory to Solid-Earth Geophysics,* Kluwer.
Sabadini, R., Yuen, D.A. & Boschi, E., 1982. Polar wander and the forced response of a rotating, multilayered, viscoelastic planet, *J. geophys. Res.,* **87,** 2885–2903.
Spada, G., 2003. *The Theory behind TABOO,* Samizdat Press, 108 pp.
Spada, G. *et al.*, 2011. A benchmark study for glacial isostatic adjustment codes, *Geophys. J. Int.,* **185,** 106–132.
Tromp, J. & Mitrovica, J., 1999. Surface loading of a viscoelastic sphere—I. General theory, *Geophys. J. Int.,* **137,** 847–855.
Tushingham, A.M. & Peltier, W.R., 1992. Validation of the ICE-3G model of the Wurm-Wisconsin deglaciation using a global data base of relative sea-level histories, *J. geophys. Res.,* **97,** 3285–3304.
Varshalovich, D.A., Moskalev, A.N. & Khersonskii, V.K., 1989. *Quantum Theory of Angular Momentum,* World Scientific Press.
Vermeersen, L.L.A. & Sabadini, R., 1996. Significance of the fundamental mantle rotational relaxation mode in polar wander simulations, *Geophys. J. Int.,* **127,** F5–F9.
Vermeersen, L.L.A., Sabadini, R., Spada, G. & Vlaar, N.J., 1994. Mountain building and Earth rotation, *Geophys. J. Int.,* **117,** 610–624.
Vermeersen, L.L.A., Fournier, A. & Sabadini, R., 1997. Changes in rotation induced by pleistocene ice masses with stratified analytical earth models, *J. geophys. Res.,* **102,** 27 689–27 702.
Wolf, D., 1991. Viscoelastodynamics of a stratified, compressible planet: incremental field equations and short- and long-time asymptotes, *Geophys. J. Int.,* **104,** 401–417.
Wu, P. & Peltier, W.R., 1982. Viscous gravitational relaxation, *Geophys. J. R. astr. Soc.,* **70,** 435–485.
Wu, P. & Peltier, W.R., 1984. Pleistocene deglaciation and the Earth's rotation: a new analysis, *Geophys. J. R. astr. Soc.,* **76,** 753–791.

APPENDIX A: PRODUCT IDENTITY

In this appendix, we prove the product identity needed for making an algebraic arrangement of eq. (114) to obtain (115). The identity has the following form:

$$\sum_{i=1}^{M-1}\frac{A_i}{s-a_i}\sum_{k=1}^{M}\frac{B_k}{s-b_k}=\sum_{i=1}^{M-1}\frac{A_i}{s-a_i}\sum_{k=1}^{M}\frac{B_k}{a_i-b_k}-\sum_{i=1}^{M}\frac{B_i}{s-b_i}\sum_{k=1}^{M-1}\frac{A_k}{a_k-b_i}, \tag{A1}$$

where $M(M\geq 2)$ is an integer number and the other symbols are real quantities. The validity of this relation will be proven by the method of mathematical induction.

In the first step of mathematical induction, we show that eq. (A1) holds for $M=2$. In this case, eq. (A1) reads as

$$\frac{A_1}{s-a_1}\left(\frac{B_1}{s-b_1}+\frac{B_2}{s-b_2}\right)=\frac{A_1}{s-a_1}\left(\frac{B_1}{a_1-b_1}+\frac{B_2}{a_1-b_2}\right)-\frac{B_1}{s-b_1}\frac{A_1}{a_1-b_1}-\frac{B_2}{s-b_2}\frac{A_1}{a_1-b_2}. \tag{A2}$$

The right-hand side of the last equation can be arranged as follows:

$$\begin{aligned}
&A_1B_1\left(\frac{1}{s-a_1}\frac{1}{a_1-b_1}-\frac{1}{s-b_1}\frac{1}{a_1-b_1}\right)+A_1B_2\left(\frac{1}{s-a_1}\frac{1}{a_1-b_2}-\frac{1}{s-b_2}\frac{1}{a_1-b_2}\right)\\
&\quad=A_1B_1\frac{(s-b_1)-(s-a_1)}{(a_1-b_1)(s-a_1)(s-b_1)}+A_1B_2\frac{(s-b_2)-(s-a_1)}{(a_1-b_2)(s-a_1)(s-b_2)}\\
&\quad=\frac{A_1}{s-a_1}\left(\frac{B_1}{s-b_1}+\frac{B_2}{s-b_2}\right),
\end{aligned}$$

which is equal to the left-hand side of eq. (A2). Thus, we have shown that eq. (A1) holds for $M=2$.

In the second step, we assume that eq. (A1) holds for a particular value M and we wish to show that it also valid for $M+1$. The left-hand side of eq. (A1) for $M+1$ can be arranged as follows:

$$\sum_{i=1}^{M}\frac{A_i}{s-a_i}\sum_{k=1}^{M+1}\frac{B_k}{s-b_k}$$

$$=\sum_{i=1}^{M-1}\frac{A_i}{s-a_i}\sum_{k=1}^{M}\frac{B_k}{s-b_k}+\sum_{i=1}^{M-1}\frac{A_i}{s-a_i}\frac{B_{M+1}}{s-b_{M+1}}+\frac{A_M}{s-a_M}\sum_{k=1}^{M+1}\frac{B_k}{s-b_k}$$

$$=\sum_{i=1}^{M-1}\frac{A_i}{s-a_i}\sum_{k=1}^{M}\frac{B_k}{a_i-b_k}-\sum_{i=1}^{M}\frac{B_i}{s-b_i}\sum_{k=1}^{M-1}\frac{A_k}{a_k-b_i}+\sum_{i=1}^{M-1}\frac{A_i}{s-a_i}\frac{B_{M+1}}{s-b_{M+1}}+\frac{A_M}{s-a_M}\sum_{k=1}^{M+1}\frac{B_k}{s-b_k}, \tag{A3}$$

where the second step is justified by the induction hypothesis that eq. (A1) holds for M. By the partial fraction decomposition,

$$\frac{1}{(s-a_i)(s-b_{M+1})}=\frac{1}{a_i-b_{M+1}}\left(\frac{1}{s-a_i}-\frac{1}{s-b_{M+1}}\right),$$

$$\frac{1}{(s-a_M)(s-b_k)}=\frac{1}{a_M-b_k}\left(\frac{1}{s-a_M}-\frac{1}{s-b_k}\right), \tag{A4}$$

the sum of the last two terms in eq. (A3) can be expressed as

$$\sum_{i=1}^{M-1}\frac{A_i}{s-a_i}\frac{B_{M+1}}{s-b_{M+1}}+\frac{A_M}{s-a_M}\sum_{k=1}^{M+1}\frac{B_k}{s-b_k}$$

$$=B_{M+1}\sum_{i=1}^{M-1}A_i\,\frac{1}{a_i-b_{M+1}}\frac{1}{s-a_i}+A_M\sum_{k=1}^{M+1}B_k\,\frac{1}{a_M-b_k}\frac{1}{s-a_M}$$

$$-B_{M+1}\sum_{i=1}^{M-1}A_i\,\frac{1}{a_i-b_{M+1}}\frac{1}{s-b_{M+1}}-A_M\sum_{k=1}^{M+1}B_k\,\frac{1}{a_M-b_k}\frac{1}{s-b_k}. \tag{A5}$$

Substituting this expression for the last two terms in eq. (A3) yields

$$\sum_{i=1}^{M}\frac{A_i}{s-a_i}\sum_{k=1}^{M+1}\frac{B_k}{s-b_k}=\sum_{i=1}^{M}\frac{A_i}{s-a_i}\sum_{k=1}^{M+1}\frac{B_k}{a_i-b_k}-\sum_{i=1}^{M+1}\frac{B_i}{s-b_i}\sum_{k=1}^{M}\frac{A_k}{a_k-b_i}, \tag{A6}$$

thereby showing that indeed, eq. (A1) holds for $M+1$. Since both inductive steps have been performed, by mathematical induction, eq. (A1) holds for all integers $M\geq 2$.